THE DESIGN OF PRESSURE VESSELS FOR EXTREME PRESSURE

by

Wayne S. Brown and S. S. Kistler

TECHNICAL REPORT
NUMBER LI
June 1, 1956

FC

OFFICE OF NAVAL RESEARCH
CONTRACT NUMBER
1288(02)
PROJECT NUMBER
NR - 052 - 357

COLLEGE OF ENGINEERING
UNIVERSITY OF UTAH
SALT LAKE CITY

THE DESIGN OF PRESSURE VESSELS FOR EXTREME PRESSURES

by

Wayne S. Brown and S. S. Kistler

INTRODUCTION

The problem of supporting extreme pressures in some kind of vessel is made difficult by the fact that materials with which the vessels might be constructed have very limited tensile strengths. This means that thick sections under tension must be used. A further, and in some ways greater limitation on supporting extreme pressures inside of vessels arises from the fact that materials with high tensile strengths when subjected to stresses tend to flow. Those materials that are highly resistent to flow under stress in general have very low tensile strengths.

The problem of research under extreme pressures is complicated by the fact that it is also necessary to have available temperatures to at least 1000°C, and preferably to twice this figure. The high tensile materials, viz., the metals, universally lose strength with rising temperature. The materials that resist high temperatures successfully are universally weak in tension. A factor of much importance is the fact that when high temperatures are to be attained inside of metal vessels the heat conductivity is so large that excessive development of heat within the vessel is required or else some form of heat insulation must be used. The heat insulating materials are almost universally weak in both tension and compression and are unsuitable for the construction of strong vessels in which high pressures may be contained.

Such considerations lead naturally to the design of composite vessels in which the outer shell is constructed of strong metals and the inner cavity is separated from the outer shell by heat and electrical insulating materials which though showing little strength in conventional tests can support high compressive loads when properly confined.

Any solid, liquid or gas if confined, can support any magnitude of pressure which might be applied to it, though its compressibility may be high and its usefulness for the construction of a pressure vessel may be negligible. In the case of a liquid or gas, we know that the distribution of an applied stress will be hydrostatic. In other words, the inter-position of a liquid or gas between an inner container for high pressures and an outer tensile shell will deliver the unit stress from the inner vessel to the outer one without loss. Such an arrangement is not uncommon in high pressure research, and as long as the outer vessel can support the outward thrust from the fluid the inner vessel will not be under a tensile stress and can contain without leakage any materials to be studied. By arranging to have hydrostatic pressure outside the inner vessel equal to the pressure within it, brittle and weak inner vessels, eg., made of glass, are found useful.

The disadvantage of such an arrangement is that the outer vessel must sustain the full unit pressure used in the inner one and for this reason pressures are limited usually to about 30,000 atmospheres.

Advantage has been taken of the fact that many materials gain greatly in strength when subjected to any large hydrostatic pressure. A small pressure vessel of cemented tungsten carbide, when immerged in a liquid at a pressure of around 30,000 atmospheres, becomes so strong that it can support internally a pressure of perhaps 100,000 atmospheres.

Very little is known of the distribution of stresses through a weak solid or through a granular material when confined and subjected to unsymmetrical stresses. For example, if the fluid in the above vessel were replaced by a powder sufficiently compacted, will the pressure from the inner vessel be transmitted to the outer one hydrostatically or will the unit pressure on the inside of the outer vessel be less than that on the outside of the inner vessel? It has sometimes been assumed that weak solids under very high pressures will hydrostatically distribute the pressure. We know of no good experimental verification except with ductile metals like lead.

If the material between the inner vessel and the outer tensile shell must be weak and incapable of supporting much tensile stress, the maximum effectiveness of this pressure transmitting material would be realized if it could support the inner load as though it were composed of a series of independent columns. Fig. 1 represents such a columnar support for the vessel. In this case the outward thrust of the columns against the outer shell will be exactly the same as the thrust from the inner vessel to the columns, whereas if the stress transmitting medium had been a fluid the outward thrust on the shell would be equal to the outward thrust

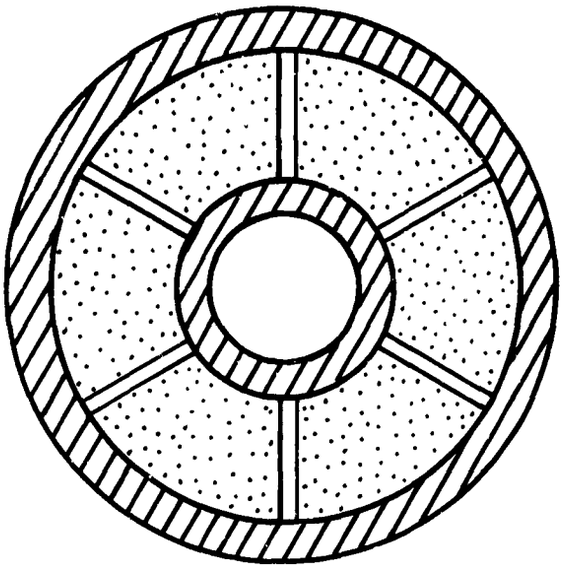

Figure 1

by the inside vessel multiplied by the ratio of the outer radius of the stress transmitting ring to its inner radius. Insofar as the intermediate ring can transmit the stress in a columnar fashion, it is effecient and may be of any desired thickness for electrical and heat insulation.

Our first study was directed to an examination of granular and weak monolithic intermediate rings to determine how stresses are transmitted through them. It seems obvious that if a material can be found that will distribute stress in a columnar manner it should be possible to design a pressure vessel capable of support any pressure desired. The only limit to the inner temperature would be the melting point of the inner vessel and the loss of columnar behavior by the intermediate material due to plastic flow.

CONCLUSIONS FROM ELASTIC THEORY

Mathematical analysis of the distribution of stresses through a solid body is in a very primitive state except for geometrically simple objects showing no flow or creep, and in which stresses never exceed the elastic limit. Unfortunately, when vessels are designed for extreme pressures it becomes impractical to stay within elastic limits and therefore only qualitative conclusions can be drawn from mathematical analysis. In spite of this limitation, a careful examination of predictions from elasticity theory can give assistance to qualitative predictions of the behavior of solids even when loaded beyond the elastic limits.

The Lamé and Clapeyron equations derived from elasticity theory, have been given numerous forms but may conveniently be represented by the following three equations:

$$\sigma_r = \frac{p_i - n^2 p_0}{n^2 - 1} - \frac{(p_i - p_0)\, n^2 a^2}{r^2 (n^2 - 1)} \qquad (1)$$

$$\sigma_t = \frac{p_i - n^2 p_0}{n^2 - 1} + \frac{(p_i - p_0)\, n^2 a^2}{r^2 (n^2 - 1)} \qquad (2)$$

$$u = \frac{1 - m}{E} \frac{p_i - n^2 p_0}{n^2 - 1} r + \frac{1 + m}{E} \frac{(p_i - p_0)\, n^2 a^2}{r (n^2 - 1)} \qquad (3)$$

where σ_r and σ_t represent the radial and tangential stresses, respectively, in a thick walled cylinder, a is the inner radius, p_i and p_0 the inner and outer pressures, r is an optional radius, u is a radial deformation, m is Poisson's ratio and E is the modulus of elasticity. The assumptions made in these three equations are that elasticity is perfect, there is no creep under stress, the modulus of elasticity remains constant regardless

of the magnitude of the compressive or tensile stress and the Poisson's ratio remains constant and independent of stress. Since these assumptions are known to be incorrect, with the possible exception of the constancy of Poisson's ratio, these equations can give only approximations. Nevertheless, they are instructive and assist one materially in design. Useful variations of these equations are those given in Equations (4), (5), and (6) where the outside pressure is zero. Here n is the ratio between the outside and inside radii and S is shearing stress. Table 1 shows how these values change with the ratio of radii.

$$\frac{S_{max}}{(\sigma_t)_{max}} = \frac{n^2}{n^2 + 1} \tag{4}$$

$$\sigma_r + \sigma_t = \frac{2\, p_i}{n^2 - 1} \tag{5}$$

$$\frac{(\sigma_t)_{mim}}{(\sigma_t)_{max}} = \frac{2}{n^2 + 1} \tag{6}$$

Table 1

n	$(\sigma_t)_{max}$	$\frac{(\sigma_t)_{min}}{(\sigma_t)_{max}}$	$\frac{S_{max}}{(\sigma_t)_{max}}$
1.01	99.00 p_i	0.99	0.505
1.11	9.55 "	.90	.53
1.25	4.55 "	.78	.65
1.43	2.92 "	.66	.67
1.67	2.12 "	.53	.74
2.0	1.66 "	.40	.80
2.5	1.23 "	.28	.86
3.33	1.20 "	.16	.92
5.0	1.08 "	.08	.96
10.0	1.02 "	.02	.99
20.0	1.00 "	.005	1.00

To see how different portions of a thick-walled cylinder contribute to the support of internal pressure, it is convenient to calculate the outward thrust at any radius by means of Equation (7),

$$T_0 = 2 p_i \int_r^{na} \sigma_t \, dr = \frac{2 (n^2 a^2 - r^{2i})}{r (n^2 - 1)} p_i . \qquad (7)$$

To illustrate the disproportionate effect of different parts of a thick cylinder, Table II has been calculated for a cylinder whose outer radius is ten times the inner radius.

Table 2

Radius	Outward Thrust
1	2 p_i
2	0.97 "
3	.61 "
4	.42 "
5	.30 "
6	.22 "
7	.15 "
8	.091"
9	.043"

It is seen from this table that the outer tenth of this thick cylinder is only 2% as effective as the inner tenth in supporting the pressure. This illustrates the fact that an increase in outer diameter of a thick-walled cylinder very quickly ceases to make any appreciable contribution to the support of the inner pressure. A cylinder 1 inch in internal diameter and 100 inches in outside diameter can support practically no more internal pressure than one that is only ten inches OD, as long as the inner fibers of the cylinder are not stressed beyond their elastic limit. To gain more

support from the outer portions of a thick cylinder, it has been common practice to stress the cylinder under internal pressure (auto-frettaging) to the point where a substantial amount of plastic flow occurs in the inner fibers. When the pressure is released the inner portion that has been distorted will be under compressive load while the outer fibers will remain under tension.

If it is desired to calculate the radial pressure within the cylinder wall at any radius, this can be obtained from the expression, $p = T_0/2r$.

Influence of Outside Support and of Poisson's Ratio. If an intermediate ring of material lies between the inner pressure vessel and the outer ring, and if it is assumed that the outer ring is perfectly rigid, one can calculate the ratio of the outward thrust at the outer surface of the intermediate ring to the outward thrust at its inner surface as

$$T_R = \frac{n p_0}{p_i} = \frac{2n}{1 + m + n^2 (1-m)} . \qquad (8)$$

In this equation Poisson's ratio, m, for the intermediate material becomes very important. At a given Poisson's ratio, the thrust ratio increases as n increases above 1, goes through a maximum and then drops toward fractional values. Table 3 shows the influence of the Poisson's ratio on the magnitude of n required to give a thrust ratio of one, and Fig. 2 represents the relation between n and T_R when $m = 0.2$.

Table 3

m	n
0	1
0.1	1.1
0.2	1.5
0.3	2.0
0.4	2.3
0.5	3.0

Figure 2

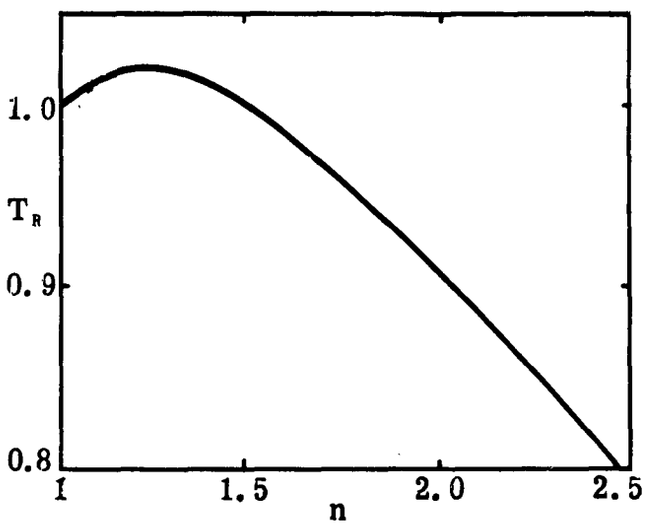

M=0.2

N	T_R
1.	1.
1.1	1.01
1.2	1.02
1.3	1.02
1.4	1.01
1.5	1.00
1.7	.97
2.0	.91
3.0	.71

Frequently, it is not sufficient to regard the outer retaining shell as completely rigid. For convenience, define a spring constant for this outer shell as $k = p_0/2u$ where p_0 is the pressure at the outside of the intermediate ring and the inside of the outer shell, and $2u$ is the deformation of the inside diameter of the outer shell. We can then obtain an equation for the thrust ratio in the intermediate ring as a function of the ratio of its radii, its Poisson ratio and its modulus of elasticity.

$$T_R = \frac{u_0}{p_1} = \frac{2n}{\frac{n^2-1}{2n}\frac{E}{ka} + 1 + m + n^2(1-m)} \quad . \qquad (9)$$

Equation (9) indicates that in order to transmit as little as possible of the thrust from the central vessel to the outer shell, it is important that the Poisson ratio be low, that the modulus of elasticity of the intermediate material be high and that the spring constant of the outer shell be low. Again it should be emphasized that these conclusions are only valid as long as elastic limits are not exceeded. It is possible, however, that with an intermediate material which normally has a low tensile strength and a low elastic limit, Equation(9) will be valid to much higher stresses in the intermediate ring than would be calculated from conventional strength data, due to the increase in strength of materials under compressive loads. In other words, if the outer shell is sufficiently strong and rigid to so support the intermediate material that it does not fail in tension, Equation(9) may be valid to high stresses. This point will be discussed further in connection with the experiments on soapstone.

Table 4

$\mathcal{E}$	T_p
0	0.72
0.5	.66
1.0	.62
2.	.54
5.	.40
10.	.28

Table 4, in which $\mathcal{E} = E/ka$, illustrates the influence of the modulus of elasticity of the intermediate material and the spring constant of the shell on the thrust ratio. For the purpose of this table, n was taken as 3 and m as 0.2. Under these conditions, if the outer tube is

perfectly rigid the thrust ratio will be 0.72. The value for this ratio is not much influenced by E/ka until it becomes greater than 1.

Conditions When The Intermediate Material Cannot Sustain Any Tensile Stress. Obviously, sand or other granular materials cannot sustain any tensile stress, although they are capable of withstanding any amount of compressive stress, as long as they can properly be supported. When packed in the annulus between an outer and an inner cylinder and loaded radially by expansion of the inner cylinder, the ends being constrained from movement, the first action will be for the grains to slide over each other, where nonradial components of forces are sufficient to overcome friction, and eventually find stable positions from which no movement will occur until stresses become so great as to fracture grains. Thus, if the internal pressure is first raised to the maximum to be studied and then backed off to a low value, the second time that the pressure is raised the granular mass should behave like an elastic solid. This solid will have an elastic modulus and a Poisson ratio dependent both upon the values for the massive solid and upon the grain shape, size and packing characteristics. Certainly we can conclude that the modulus of elasticity of the granular mass will be lower than that of the massive material, but it is not so clear how Poisson's ratio will be influenced.

Prevention of longitudinal movement of the granular mass will cause some deviation from the basic Lamé and Clapeyron equations and this subject should be investigated carefully. A hasty estimation of such deviations indicates that it will usually be less than 10%.

Figure 3

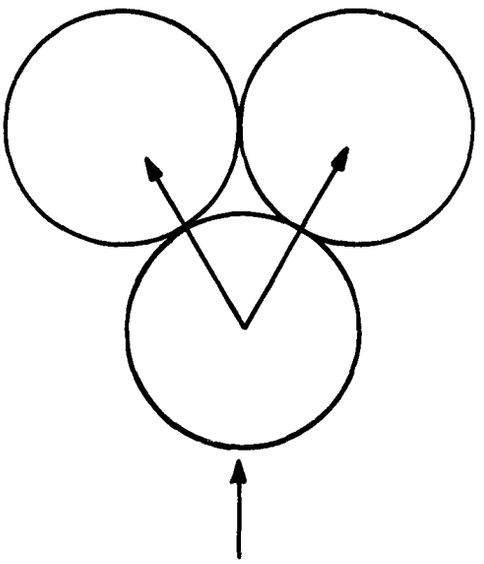

It might be remarked here that the customary calculations of stresses between rings shrunk together do not make allowance for the longitudinal friction between these rings.

If we think of the granules as being spherical as in Fig. 3, it is easy to see how there must be a lateral component of thrust when force is applied to any granule. The magnitude of this lateral thrust must be a function of the type of packing, the Poisson expansion and the coeficient of friction between the grains. Assuming spheres of equal diameter and with a specific packing geometry, some analytical conclusion on the magnitude of the lateral thrust would be possible. If sizes, shapes, and packing relationships are random as would be expected in a crushed material, analytical effort would be unrewarding. At least we can conclude that, as long as movement does not occur during a measurement, the lateral thrust must be proportional to the applied force.

In the case of a cylinder of the granular mass held between an outer retaining cylinder and an inner elastic cylinder through which the force is applied, as in Fig. 1, the outward thrust at any radius must be given by

$$T_0 = 2p_i r_i + 2\int_{r_i}^{r} \sigma_t \, dr.$$

When the lateral thrust is proportional to the applied force,

$$\sigma_t = \frac{gT_0}{2r} \quad \text{and}$$

$$T_0 = \frac{2\sigma_t r}{g} = 2p_i r_i + 2\int_{r_i}^{r} \sigma_t \, dr \ .$$

Here g is a proportionality constant. Differentiating,

$$\frac{\sigma_t}{g} dr + \frac{r}{g} d\sigma_t = \sigma_t \, dr$$

which, when like terms are collected, integrates to

$$(1-g) \ln r = -\ln \sigma_t + c. \tag{10}$$

Introducing the boundary conditions that when $r = r_i$, $T_0 = 2p_i r_i$ and when $r = r_0$, $T_0 = 2p_0 r_0$

$$(1-g) \ln \frac{r_i}{r_0} = \ln \frac{p_0}{p_i} \tag{11}$$

or

$$g = \frac{\ln \frac{r_0}{r_i} - \ln \frac{p_i}{p_0}}{\ln \frac{r_0}{r_i}} \tag{12}$$

Experimental studies of granular materials will be given later.

The Tensile Shell. Regardless of the means of distributing the outward thrust from the inner vessel, it all must be held together by the

outer tensile member, which in all cases must be thick in order to support the very large loads. As illustrated above in Table 2, the effectiveness of a thick-walled cylinder or sphere in supporting high internal pressures is increased to a rapidly diminishing extent by increase in thickness. In cases in which extensive plastic deformation can be permitted, the stress distribution characteristic of elastic vessels can be changed to one in which the fiber stresses are more uniform throughout the thickness of the vessel and therefore added thickness is effective more nearly in proportion to the thickness. Unfortunately, steels that can be deformed to this extent must be relatively ductile and as a consequence do not have a high tensile strength, while conversely the steels with very high tensile strength are only slightly ductile. For most effective use of steel it becomes necessary to stress artificially different layers of the outer shell so that the resultant will be a vessel that can support a maximum pressure. This pre-stressing may be done by wrapping square steel wire or steel strap around a hardened core, tensioning it suitably as it is wrapped, or by shrinking several shells together. The object is to put the inner layers in compression and the outer layers in tension so that when the vessel is elastically distorted by internal pressure the whole cross section will be approximately uniformally stressed.

If pressure is to be maintained for long periods within the vessel, it is not desirable to stress any part of the shell beyond its elastic limit because of the creep of metal at such stresses.

Assume that the maximum stress to which any fiber may be subjected is $(\sigma_t)_{max}$. Equation (13) then gives the relationship between it the mean stress throughout a ring and n.

$$(\sigma_t)_{ave} = \frac{1}{(n-1)a} \int_a^{na} \frac{(\sigma_t)_{max}}{n^2 + 1} \left(1 + \frac{n^2 a^2}{r^2}\right) dr$$

$$= (\sigma_t)_{max} \frac{n+1}{n^2+1} \quad . \qquad (13)$$

It is evident that, for a high mean stress in the steel, n must be close to 1, which means that for a thick vessel the rings must be thin. Wire winding would therefore be ideal if it were not for longitudinal weakness and for mechanical difficulties in the winding process. Shrinking of shells together is practical for vessels to support high internal pressure. To illustrate the advantages of several shells, it was postulated that the maximum tensile stress to which steel in a pressure vessel can be subjected is 150,000 lbs. per square inch. The outside diameter of the vessel was taken as 3 inches and the ID as one half inch. Table 5 and Fig. 4 show the effect of increasing the number of rings from one to ten.

Table 5

Number of rings	n	$(\sigma_t)_{ave}$
1	6	28,400 psi
2	2.45	74,000
3	1.82	98,100
4	1.56	111,500
5	1.43	120,000
7	1.29	129,000
10	1.20	136,000

Figure 4

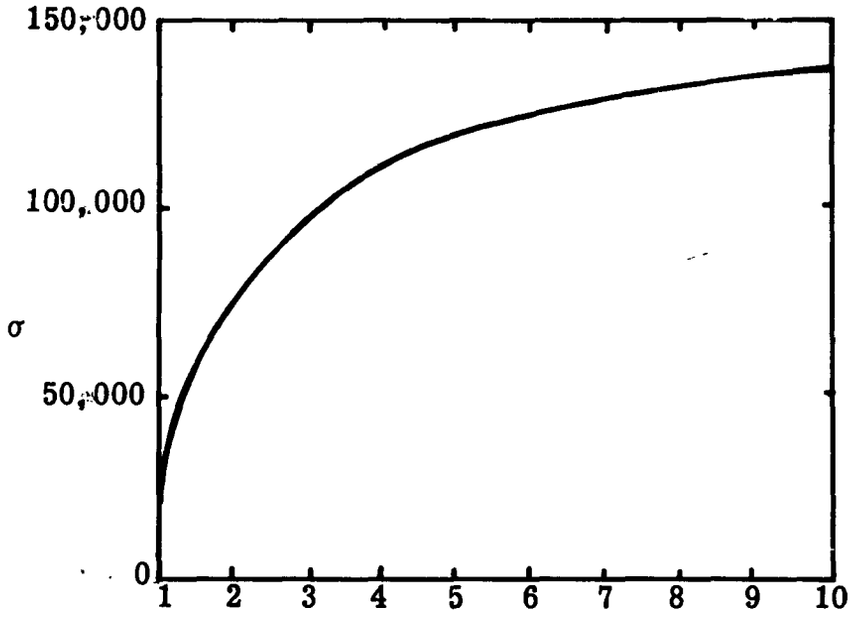

N	$(\sigma_t)_{ave.}$
1	28,400
2	74,000
3	98,100
4	111,500
5	120,000
7	129,000
10	136,000

N = number of rings

In machining rings for assembly, it is convenient to calculate in advance the dimensions of each ring. The inside and outside deformations of any particular ring, f, in an assembly can be calculated by means of Equations (14) and (15):

$$u_1 = \frac{(\sigma_t)_{ave}\, n^{f-1}\, a}{E(n^2-1)}\left[(1-m)(n^2-1+n^{N-f+1}-n^{N-f+2})+(1+m)\right.$$
$$\left.(n^{N-f+3}-n^{N-f+2})\right] \qquad (14)$$

$$u_0 = \frac{(\sigma_t)_{ave}\, n^{f}\, a}{E(n^2-1)}\left[(1-m)(n^2-1+n^{N-f+1}-n^{N-f+2})+(1+m)\right.$$
$$\left.(n^{N-f+1}-n^{N-f})\right] \qquad (15)$$

where u_1 and u_0 are the deformations of the inside and outside radii, resp. and N is the total number of rings.

In these equations the assumption is made that the rings are shrunk onto a rigid, non-yielding core. Of course, the pressure on this rigid core will be

$$p_c = (\sigma_t)_{ave} \frac{(n-1)a}{a} = (\sigma_t)_{ave} (n-1) .$$

Maximum pressures thus achieved can be greater than 30,000 atmospheres, limited mainly by the creep of the inner steel ring under its high compressive load.

Support of High Compressive Loads. Up to this point we have been concerned only with the retention of high pressures inside of a vessel. Nothing has been said about how the pressure has been generated in this vessel nor what sort of closures may be used. Some consideration should be given to the support of high compressive loads on pistons or the like. If we subject a solid cylinder to compression in a testing machine, at some compressive stress it will fail, usually by sheer. Sometimes failure occurs by a tensile break along planes parallel with the direction of loading producing "barrelling". The extensive work of Bridgman has shown clearly that the compressive strength of all solids is increased greatly by hydrostatic pressure. Instead of providing hydrostatic pressure around a piston, we might support it in a rigid tube so that no lateral sheer can occur, Fig. 5. Provided that the surrounding cylinder is perfectly rigid and has limitless strength, the piston can support limitless load. This is merely another aspect of the support of internal pressure by means of a ring of material adequately backed up

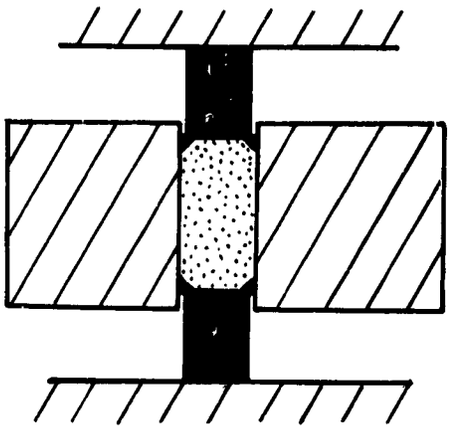

Figure 5

on the outside. Under the above postulated conditions, the material of which the piston is made is of little importance. Practically, neither a perfectly rigid tube nor one that can support limitless pressure is possible, and the material of the piston is of great importance.

To gain knowledge of the lateral pressure that one should expect from a piston loaded in compression and supported by a perfectly rigid tube, an analysis was made which led to an infinite series that converges to the simple expression in Equation (16)

$$P = \frac{m}{1 - m} \; p_o \tag{16}$$

$$\text{shortening} = \frac{p_o}{E}\left(1 - \frac{2\,m^2}{1 - m}\right) \tag{17}$$

where P is the lateral pressure and p_o is the pressure applied to the ends of the piston. Frictionless support was postulated, and of course

constancy of Poisson's ratio. Table 6 shows the influence of m on both shortening and lateral pressure.

Table 6

m	Shortening	p
0.5	0.0	1.0 p_e
0.4	.467 p_e/E	.67 "
0.3	.743 "	.43 "
0.2	.900 "	.25 "
0.15	.947 "	.18 "
0.1	.978 "	.11 "

A similar analysis of the more realistic situation in which a piston is supported by an elastic tube, which may have been shrunk on with a given shrink interference i leads to Equation (18) which, when i = 0 and k is indefinitely large, reduces to (16).

$$\Delta d = \frac{p_e}{E} me - i(1-e) + \frac{B}{1-m^2(1-e)^2} \qquad (18)$$

where $B = \frac{p_e}{E} me(1-e)[m + m^2(1-e)] + ime(1-e) + im^2e(1-e)^2$

d is the diameter, taken as 1, $e = E/k + E$ and i is the shrink interference on the diameter. The spring constant, k, has the same meaning as formerly. E is the modulus of elasticity of the piston material. The lateral pressure, P, is obtained from $P = k\Delta d$.

Spring Constant of a Tube, when pressure is applied to the inside only, is found from Eq. (3) and $k = p_i/\Delta d_i$. Table 7 shows the way k changes with thickness of the walls of the tube when it is made of steel with $E = 30 \times 10^6$ psi and when it is made of Carboloy with $E = 95 \times 10^6$

psi. Poisson's ratio for steel is 0.25 and for this grade of Carboloy is 0.17. The inside diameter of the tube was taken as 0.25 inch for these calculations.

Table 7

n	k_{steel}	$k_{carbo.}$
1.1	1.12×10^7 psi	0.36×10^8 psi
1.2	2.07 "	---
1.4	3.61 "	1.17×10^8 psi
1.7	5.25 "	---
2.0	6.25 "	2.06 "
3.0	8.0 "	---
4.0	8.7 "	2.92 "
6.0	9.2 "	---
∞	9.6 "	3.25 "

It will be seen from this table that the spring constant increases relatively little when the outside diameter increases beyond twice the inside diameter. In other words, the rigidity of the tube to inside pressure becomes independent of the wall thickness at small values of n. There is, then, no virtue in supporting the piston with a ring many times its diameter unless there are other factors than k that contribute to the support.

Since rigidity of the support is obviously desirable, a composite of an inner tube of Carboloy shrunk onto the piston and a ring of steel shrunk onto the Carboloy was investigated. It was found that

$$k = \frac{(n^2-1)E}{2a} \cdot \frac{1}{n^2(1+m) + 1 - m - \frac{4n^2 k_s}{G}} \qquad (19)$$

where $G = \frac{(n^2-1)E}{2an} + k_s [n^2(1-m) + 1 + m]$.

In these expressions n, m and E take the values for Carboloy while k_s is the spring constant of the steel ring surrounding the Carboloy tube.

A numerical example in which the Carboloy tube is 1/2 inch OD and 1/4 inch ID and is surrounded by a steel ring 3 inches OD shows that $k = 28.4 \times 10^7$ psi whereas with no steel at all $k = 20.6 \times 10^7$ psi. Any large advantage due to the steel band cannot be attributed to increased stiffness.

There is doubtless great value in putting the piston under initial high lateral compression so that great end pressure can be supported before lateral expansion can occur of sufficient magnitude to cause fracturing of the piston. At present it is not known how fracturing will influence the lateral pressure developed, but it seems unlikely that it will reduce it. Doubtless, fracturing will be most apt to occur at the ends where support may not be as uniform as in the center and where failure will be least desirable.

Mr. Claire Coleman is investigating the relationship of lateral support of piston materials, by rings of steel shrunk onto them, and the occurrence of fracturing on end loading. It seems probable that for any given piston material there is a shrink interference and a spring constant of the surrounding ring that will prevent fracture at any pressure short of one producing plastic distortion or failure of the ring.

EXPERIMENTS WITH A HOLLOW SOAPSTONE CYLINDER LOADED INTERNALLY.

A cylinder of soapstone three inches OD, 0.822 inches ID and

12 inches long was turned from a solid block of "Lava" obtained from the American Lava Company. Their description of this particular grade is that it is a hydrated aluminum silicate. Our own measurements on small specimens show that it is not entirely isotropic, the compressive strength varying from 4200 psi to 5400 psi when measured in different directions in the block. This cylinder of soapstone was fitted into a steel cylinder 3 inches ID with a 1/4 inch wall thickness and assembled in the apparatus of Figure 6. A more detailed description of the apparatus will be found under Experiments with Granular Material. Two SR-4 strain gauges, located on opposite sides of the steel cylinder and half-way between the ends, were used to measure the outward thrust of the soapstone against the steel cylinder. In the first run the internal pressure was raised in steps of 1000 lbs. per square inch to 8,000 psi at which pressure the copper tubing failed. A second cycle in which the pressure was raised in the same steps to 6,000 psi and then backed off again gave a decided hysteresis loop, as did both of the runs of Dec. 30 in which 7000 psi was reached.

After replacing the copper tube with stainless steel, the data of Feb. 4 were taken, reaching a maximum pressure of 10,000 psi. Table 8 gives the results of these tests. The data of Feb. 4 are plotted in Fig. 7. The strains indicated are averages of the two measured at diametrically opposite points. The two strain gauges differ substantially in their readings, probably indicating anisotropic behavior of the soapstone

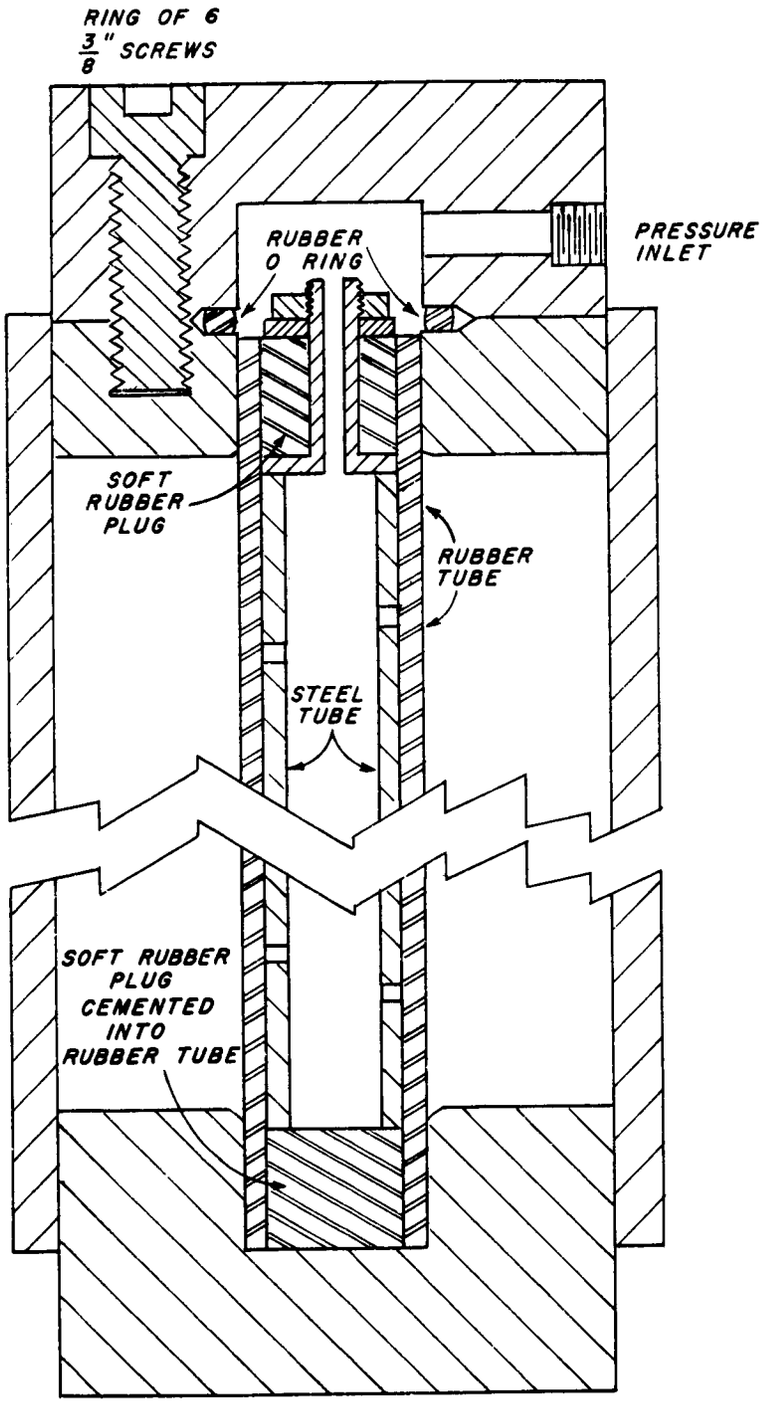

SKETCH OF APPARATUS USED IN TESTS WITH AGGREGATE MATERIALS.

FIGURE 6

Table 8

Strain in the Steel vs. Internal Pressure in the Soapstone

Dec. 22		Dec. 23		Dec. 30		Dec. 30		Feb. 4	
Press.	Strain	Press.	Strain	Press.	Strain	Press.	Strain	Press.	Strain
1000 psi	14 μ in/in	1000 psi	12 μ in/in	1000 psi	15 μ in/in	1000 μ in/in	15 psi	1000 psi	11.5 μ in/in
2000	31	2000	28	2000	30	2000	30	2000	26
3000	49	3000	46	3000	48	3000	48	3000	48
4000	62	4000	74	4000	76	4000	75	4000	72
5000	88	5000	103	5000	110	5000	109	5000	107
6000	156	6000	146	6000	150	6000	148	6000	141
7000	208	5000	118	7000	188	7000	187	7000	172
8000	284	4000	89	6000	156	6000	156	8000	232
		3000	63	5000	126	5000	124	9000	282
		2000	38	4000	95	4000	92	10000	325
		1000	15	3000	63	3000	62	4000	106
		0	-1	2000	38	2000	37	2000	33
				1000	16	1000	16	5000	102
				750	12	750	--	6000	140
				500	6	500	10	7000	182
				100	0	100	6	8000	222
						0	-2	9000	271
								10000	322

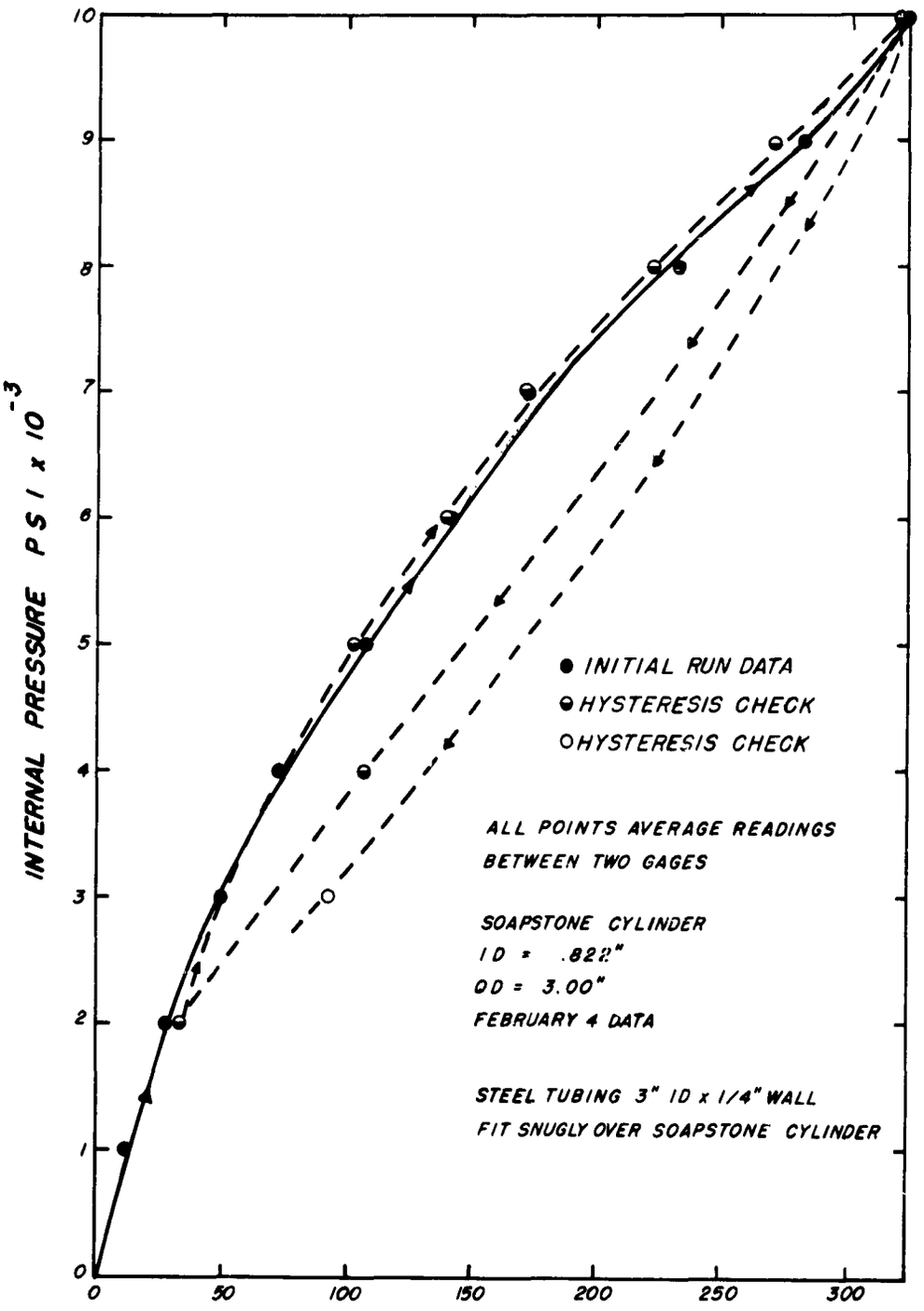
INTERNAL PRESSURE PSI x 10^-3
STRAIN IN OUTER FIBERS OF STEEL (MICRO INCHES/ INCH)
0
1
2
3
4
5
6
7
8
9
10
0
50
100
150
200
250
300
● INITIAL RUN DATA
◒ HYSTERESIS CHECK
○ HYSTERESIS CHECK
ALL POINTS AVERAGE READINGS BETWEEN TWO GAGES
SOAPSTONE CYLINDER
ID = .822"
OD = 3.00"
FEBRUARY 4 DATA
STEEL TUBING 3" ID x 1/4" WALL
FIT SNUGLY OVER SOAPSTONE CYLINDER

FIGURE 7

cylinder. The figures show good duplication of results inspite of hysteresis. All calculations were made on data taken with increasing pressure.

On disassembling the apparatus, the soapstone cylinder was found cracked longitudinally into two approximately equal halves. We have no knowledge of when this crack occurred since there was neither sound nor a break in any of the curves to indicate it.

Table 9

p_i	Ave. Strain in Steel	Thrust		T_R
		Steel	Inside	
1000	11.5 μ in.	186	822	0.23
2000	26.5 "	429	1640	.26
3000	48	777	2470	.32
4000	72	1165	3300	.35
5000	107	1730	4100	.42
6000	141	2285	4900	.47
7000	172	2780	5800	.48
8000	232	3760	6600	.57
9000	282	4560	7400	.62
10000	325	5260	8200	.64

Table 9 gives an analysis of the outward thrust against the steel cylinder, the thrust inside of the soapstone cylinder and the ratio between these thrusts for the run of Feb. 4. The last column shows clearly that the transmission of thrust by the soapstone to the steel cylinder increases almost three-fold between 1000 and 10,000 lbs. per square inch internal pressure. Nevertheless, it is rather remarkable that such a soft and weak material as soapstone with a compressive strength of only 5000 psi and

a tensile strength undoubtedly much below this figure withstood the outward thrust as successfully as it did. Were it behaving in a purely columnar fashion the thrust ratio would be 1. It is interesting to speculate how the soapstone has so effectively resisted the internal thrust when it was cracked into two pieces.

Equation (9) gives the behavior to be expected from an elastic body. Substituting $n = 3.65$, $m = 0.2$, $E = 2.6 \times 10^6$, and $k = 1.67 \times 10^6$ into this equation one obtains a thrust ratio of 0.40. Obviously the soapstone cylinder is not acting as an elastic body, but it is interesting to note that the calculated thrust ratio lies about in the center of the range observed. The values for E and m were obtained from measurements on specimens, cut from the same block of soapstone, stressed in compression. The steady increase in the thrust ratio with internal pressure probably indicates yielding in the inner layers of stone. If this is so, it is remarkable that, on restressing, the same behavior is again observed. It may be that at the higher pressures the inner layers of soapstone yield by shearing without failure, and one release of the pressure reverse shearing occurs. The steady increase in thrust ratio with internal pressure would then be attributed to the occurrence of shearing, perhaps at relatively constant shearing stress, outward from the hole to longer and longer radii. The mathematical treatment of such a mechanism would be relatively simple but has not been undertaken here due to the split in the cylinder and the doubtful value of any analysis. If this is what is occurring, it seems strange that so little

residual stress remains on dropping the internal pressure to zero.

Conclusions would have been safer had we been able to go to internal pressures several times as high as the maximum attained. Nevertheless, it is instructive to note that even such a soft material as soapstone can support large pressures without transmitting them in any way resembling hydrostatic distribution, as has been surmised by some. Data to be presented in a later report will show that even under 300,000 psi soapstone, when confined, transmits pressure as an elastic solid and is just as far from behaving like a fluid as in the experiments above.

EXPERIMENTS WITH GRANULAR MATERIALS

As pointed out earlier, a confined solid can support unlimited pressure as long as the container does not yield. It is, however, possible that the solid transmitting the pressure may fragment. We had postulated that in the case of brittle solids like soapstone there would be a zone near the center that would fail by shear, the failure extending as a fragmented zone outward to a distance dependent upon the total internal pressure and the shearing strength of the solid cylinder. Attempts were made to use plaster-of-Paris by casting it into the apparatus of Fig. 6 since it is well known to fail without much plastic flow. The extensive trials with plaster did not yield sufficiently consistent results to report here. It was for this reason that we resorted to soapstone which is so dense as not to crush due to internal collapse of the pores. Unfortunately, the ability of soapstone to shear under confinement prevented us from

observing the phenomenon that we still believe would occur with a brittle material under sufficiently large internal pressure.

Since a fragmented solid would possess no tensile strength, its behavior as a pressure transmitting medium must be different from that of a continuous solid, and it has been postulated by some that a powder will, at sufficiently high pressures, transmit stress hydrostatically. It became important to examine granular material under load. A wide variety of kinds was studied in the hope of finding some relation between behavior under load and other properties.

The apparatus used was the same as that employed with soapstone and plaster. The granular material was packed densely in the annulus surrounding the rubber tube of Fig. 6. A perforated metal tube inside the rubber prevented its collapse during the packing. Pressure was applied by means of water from a pump capable of 10,000 psi. The thrust transmitted to the shell was measured by SR-4 strain gauges as previously.

End movement of the top and bottom plugs was prevented by placing the apparatus in a compression testing machine, placing 3 - 1 1/4 inch diamter steel rods of the same length as the apparatus as stops between the platens of the machine and applying 30,000 pounds load to the rods. Thus any movement of the plugs would involve springing the testing machine. It was so arranged that up to 5000 lbs. was applied directly to the plugs. The rigidity of this set-up proved entirely adequate. Maximum observed change in length was 0.0015". The steel shell was supported

by small blocks until pressure was applied, after which it showed no tendency to slip down.

The method of running a test was as follows. The bottom end plug containing the rubber tube was mounted in the steel cylinder. The granular material was then packed between the cylinder and the rubber tube. Several methods of packing the granular material were attempted. The one that seemed most satisfactory and that was used in most of the tests was to pour the material in place with the cylinder mounted on a small jolting table of the type used in foundries for making small sand molds. The table rises and falls vertically while simultaneously being vibrated in a horizontal plane. After filling the cylinder to the proper level the inner top plug was installed. The pressure seal which prevents the fluid from leaking between the steel and the rubber tube can be seen in the figure. A rubber stopper was ground round and a hole drilled through its center. A small steel bolt with a hole drilled through its longitudinal axis was inserted through the stopper. By tightening a nut placed on the bolt the rubber stopper was forced to expand forcing the rubber tube against the steel. The upper cap was then bolted in place using a rubber O ring for a seal.

After the apparatus was situated in the machine and the end load applied, the SR-4 strain gauges were connected to the indicator and an initial reading for each gauge was obtained. As internal pressure was applied, strain gauge readings were taken at various intervals as the

pressure was increased. After reaching the peak pressure, readings were taken as the pressure decreased to obtain hysteresis effects.

One of the important measurements needed for the analysis of test results was the inside diameter of the granular cylinder (soft rubber in this situation behaves hydrostatically). One possible way of obtaining this that appeared plausible was to carefully disassemble the apparatus after the test and measure the diameter of the wall taking advantage of the material's packing properties. This proved to be unsuccessful for most of the materials used since there was not sufficient packing to provide a well defined inner surface. Several other methods were attempted with about the same success. The method which proved quite successful was to place a radioactive cobalt source on one side of the cylinder and a photographic plate on the other. The pressure was maintained at the desired value while the exposure was made. See Fig. 8. This is essentially the same technique as industrial X-ray equipment uses except in this case the gamma rays have a higher energy than X-rays. With proper exposures it was possible to obtain well defined lines indicating the inner wall of the granular cylinder. Figure 9 is a reproduction of a typical picture. This was made with a 1 1/2 curie cobalt 60 source and an exposure of 45 minutes. Upon close examination the steel perforated tube, the rubber tube, the granular cylinder, and the steel cylinder are all evident. It is obvious from Fig. 8 that the hole diameter shown on the photographic plate is larger than the actual hole and has to be corrected for geometry.

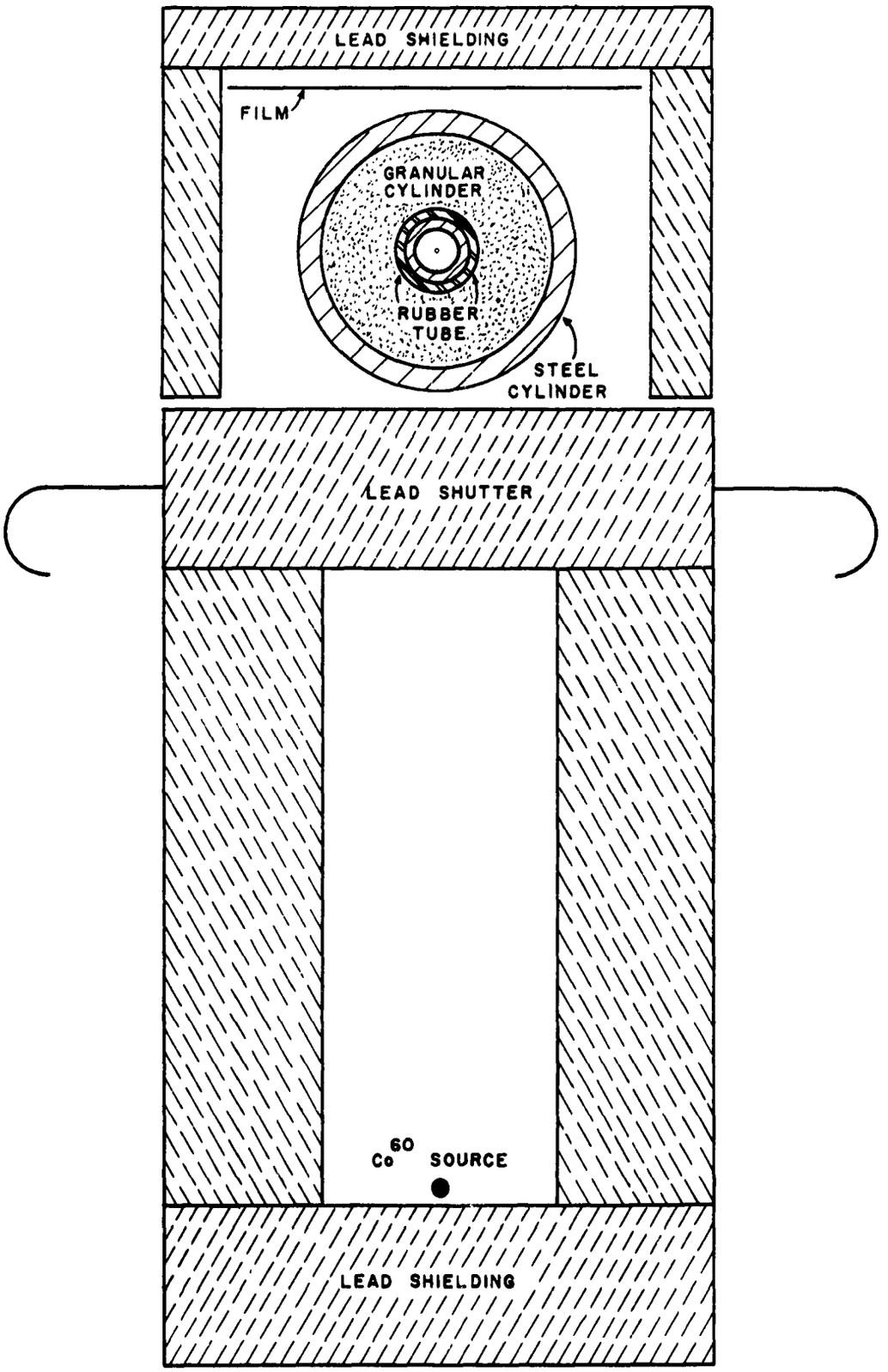
LEAD SHIELDING
FILM
GRANULAR CYLINDER
RUBBER TUBE
STEEL CYLINDER
LEAD SHUTTER
Co^{60} SOURCE
LEAD SHIELDING

FIGURE 8

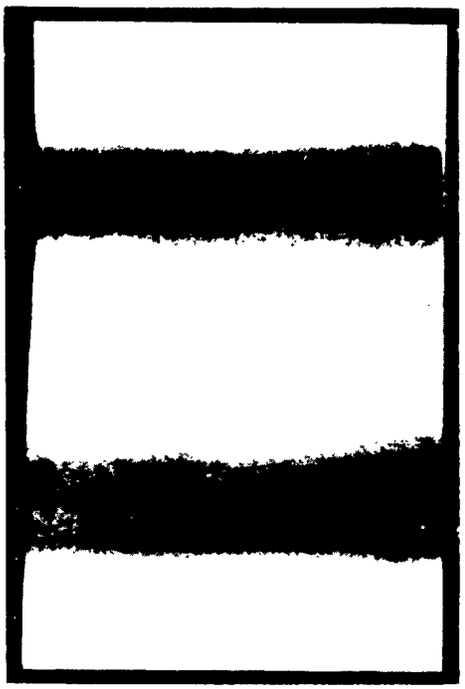

Figure 9

This correction factor is simply the ratio of the distance from the source to the center of the hole divided by the distance from the source to the film. A calibration picture made by placing a steel rod of known diameter in the same geometrical position as the hole proved the correction to be accurate. Tests of this type were made with some of the granular materials and with cylinders of different sizes. It now appears unfortunate that this technique was not developed earlier.

Ottawa Sand. The first material tested was 20-30 mesh Ottawa sand. This is a silica sand with nearly spherical particles about 750 microns in diameter. As the pressure was increased with this sand in

the apparatus, audible cracking was heard beginning at about 3000 psi and continuing for the duration of the test. Upon disassembly, the inner wall of the sand was sufficiently packed to obtain a fair reading of the inside diameter with a Tee type inside micrometer. Samples of sand were taken near the inner and outer walls and at two intermediate radial positions. These were viewed under a stereo microscope. It was observed that the sand near the inner wall was crushed badly, there remaining very few whole particles. The average particle size was about 75 microns or one tenth the original size. The sand taken from a position about 1/4 inch from the inner wall showed the same results with even fewer whole particles. The samples taken further from the center all showed more unbroken particles and less crushing (i.e., larger fragments) than the inner samples.

The sand tests were made using a steel cylinder 12 inches long, with 3 inch inside diameter and a 0.255 inch wall. Two rubber tubes were used in the sand tests with outside diameters of 0.90 inches and 0.81 inches. The steel cylinder had two strain gauges placed at the center and one at each end about 1 inch from the end plug to determine differences due to end effects. It was found that the end effect was not significant. Figure 10 is the graph of the internal pressure and the strain gauge readings. The hysteresis effect as checked by one of the center gauges is also shown.

Figure 11 shows the same type of plot starting with new sand and

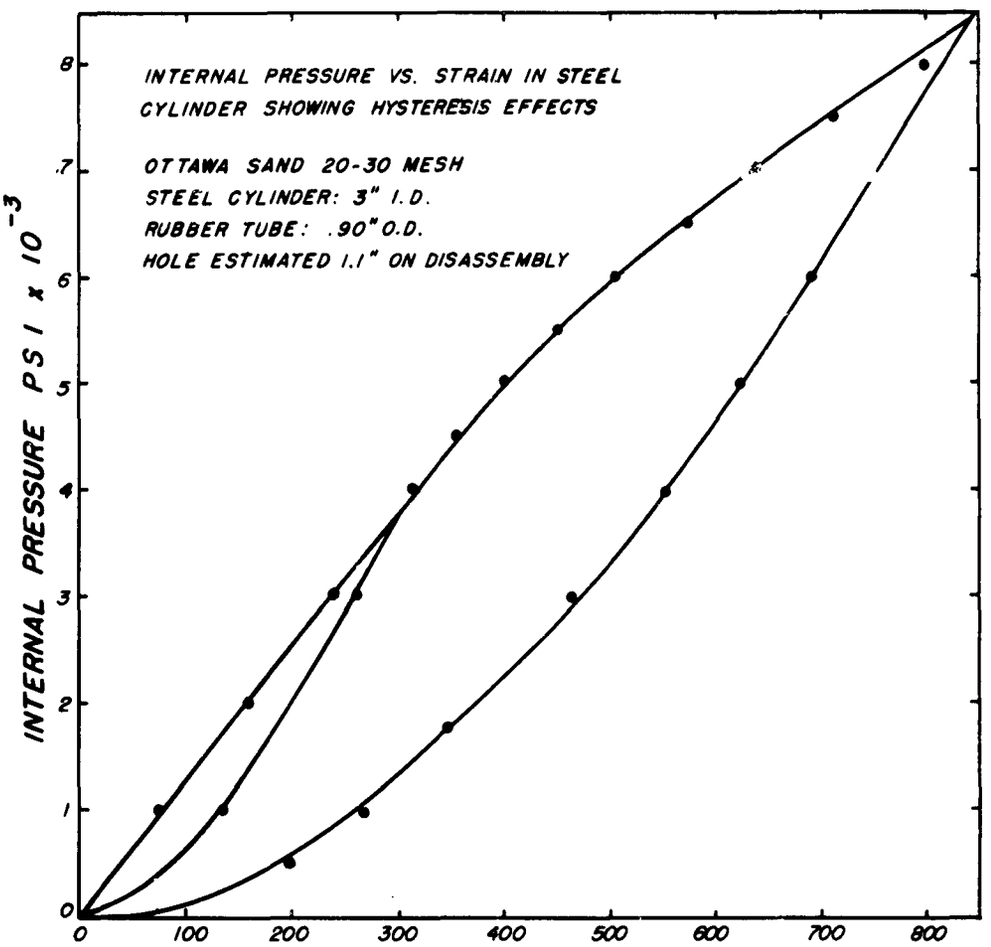
INTERNAL PRESSURE VS. STRAIN IN STEEL
CYLINDER SHOWING HYSTERESIS EFFECTS
OTTAWA SAND 20-30 MESH
STEEL CYLINDER: 3" I.D.
RUBBER TUBE: .90" O.D.
HOLE ESTIMATED 1.1" ON DISASSEMBLY
INTERNAL PRESSURE PSI x 10^-3
0
1
2
3
4
5
6
.7
8
0
100
200
300
400
500
600
700
800
STRAIN (MICRO INCHES / INCH)

FIGURE 10

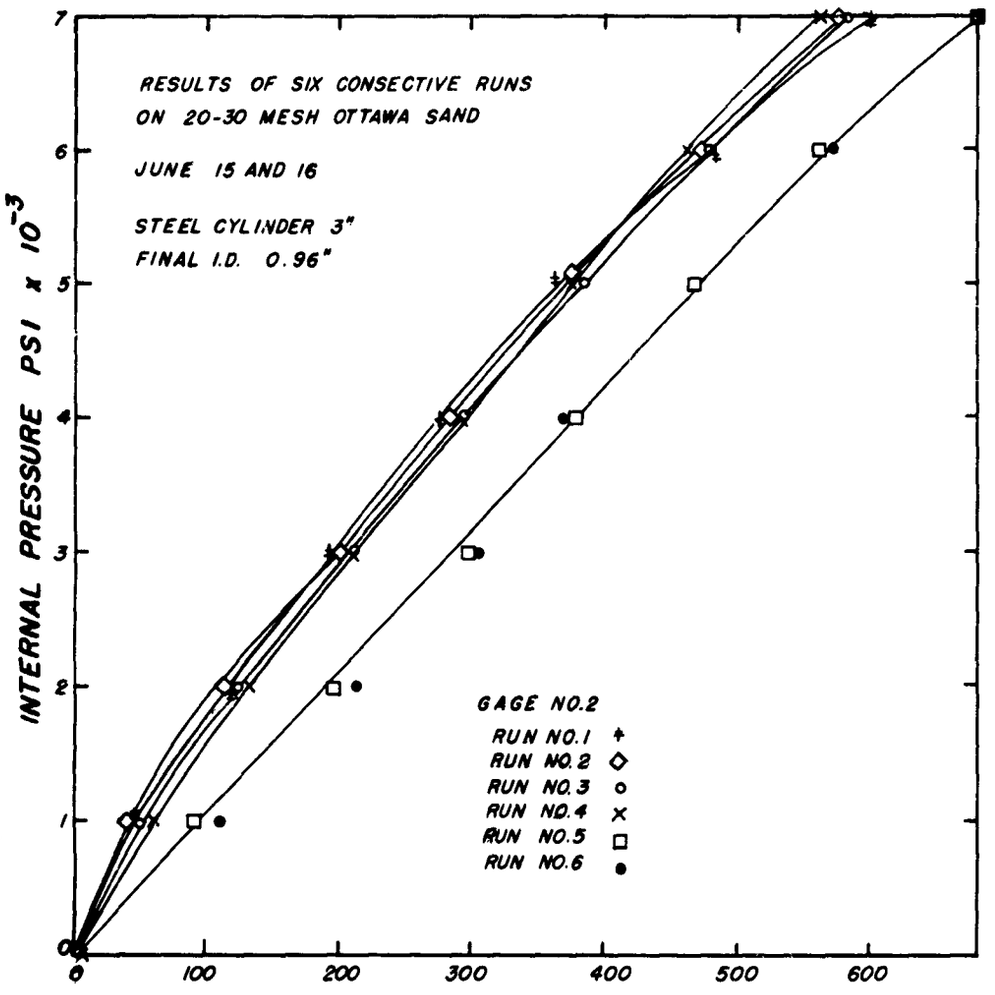
RESULTS OF SIX CONSECTIVE RUNS
ON 20-30 MESH OTTAWA SAND
JUNE 15 AND 16
STEEL CYLINDER 3"
FINAL I.D. 0.96"
GAGE NO.2
RUN NO.1
RUN NO.2
RUN NO.3
RUN NO.4
RUN NO.5
RUN NO.6
INTERNAL PRESSURE PSI x 10^{-3}
STRAIN (MICRO INCHES / INCH)
0
1
2
3
4
5
6
7
0
100
200
300
400
500
600

FIGURE 11

repeating the test six times, omitting observations on hysteresis. It is noted that the first four tests showed excellent agreement and that the last two tests while somewhat different from the first four agree well with each other. Failure of the rubber tube prevented further checking of this difference in results.

Glass Beads. Glass beads produced by The Minnesota Mining and Manufacturing Company for pavement marking were obtained in two sizes and tested. The larger beads were almost perfect spheres 65 to 75 microns in diameter. Observation with a stereo microscope after testing showed that many beads had shattered into fragments about one tenth their original size. The smaller beads were spherical with a diameter of 3 to 6 microns and showed very little crushing from the pressure. Figure 12 shows the results of tests made with the glass beads. It may be noted that there is more variation with consecutive tests on coarse beads than with the fine beads. This is probably due to crushing the former.

Alumina. Test results from a test using 8 - 14 mesh white alumina abrasive are shown in Figure 13. This test was made using a 5 inch ID steel cylinder with a 1/4 inch wall. The rubber tube had an initial OD of 1 1/4 inches. After testing, the alumina was well packed on the inner wall and the diameter was 1.62 inches. Samples were examined under a microscope and it was observed that most particles were broken with no apparent difference due to the location in the cylinder.

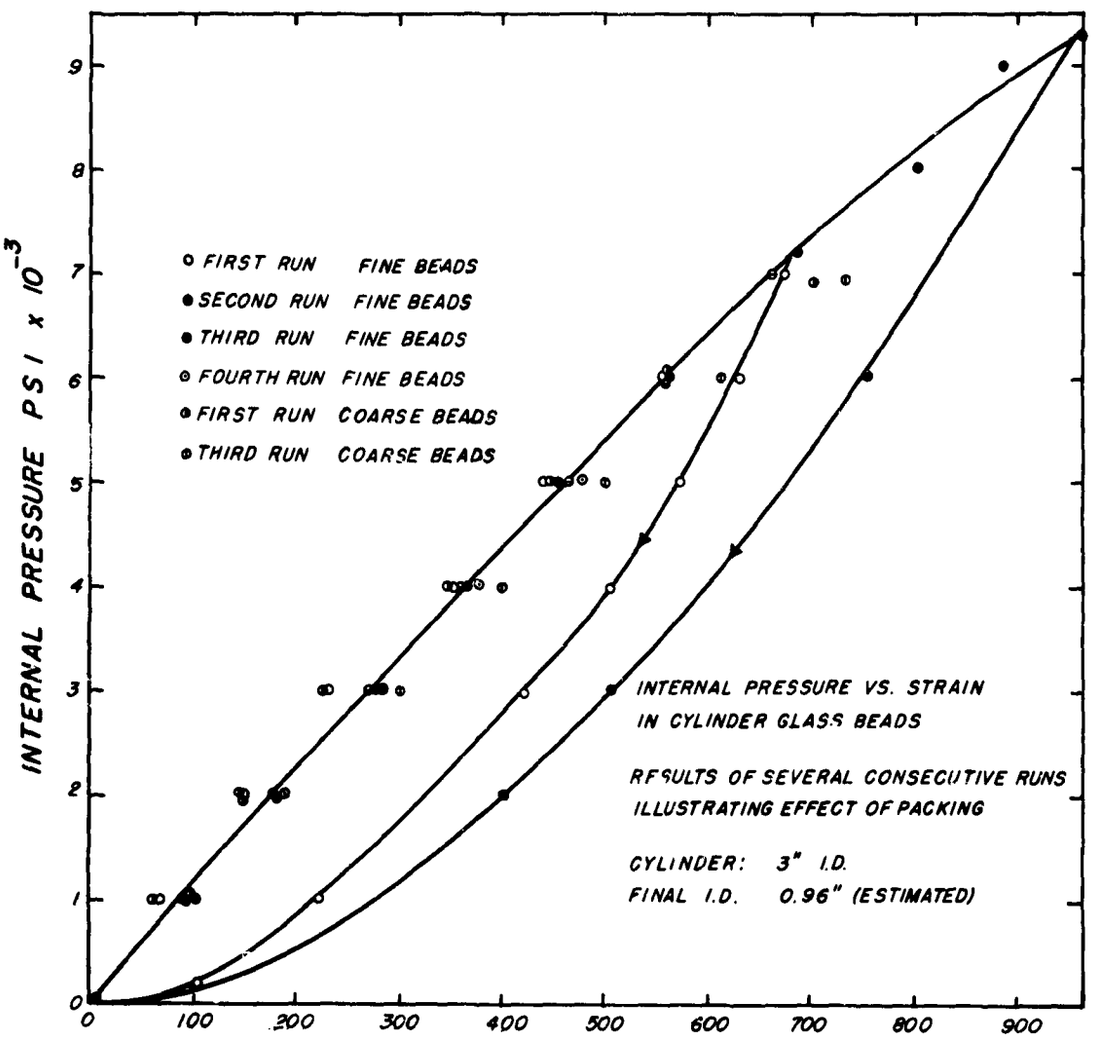
INTERNAL PRESSURE PSI x 10^{-3}
STRAIN (MICRO INCHES / INCH)
0
1
2
3
4
5
6
7
8
9
0
100
200
300
400
500
600
700
800
900
FIRST RUN FINE BEADS
SECOND RUN FINE BEADS
THIRD RUN FINE BEADS
FOURTH RUN FINE BEADS
FIRST RUN COARSE BEADS
THIRD RUN COARSE BEADS
INTERNAL PRESSURE VS. STRAIN
IN CYLINDER GLASS BEADS
RESULTS OF SEVERAL CONSECUTIVE RUNS
ILLUSTRATING EFFECT OF PACKING
CYLINDER: 3" I.D.
FINAL I.D. 0.96" (ESTIMATED)

FIGURE 12

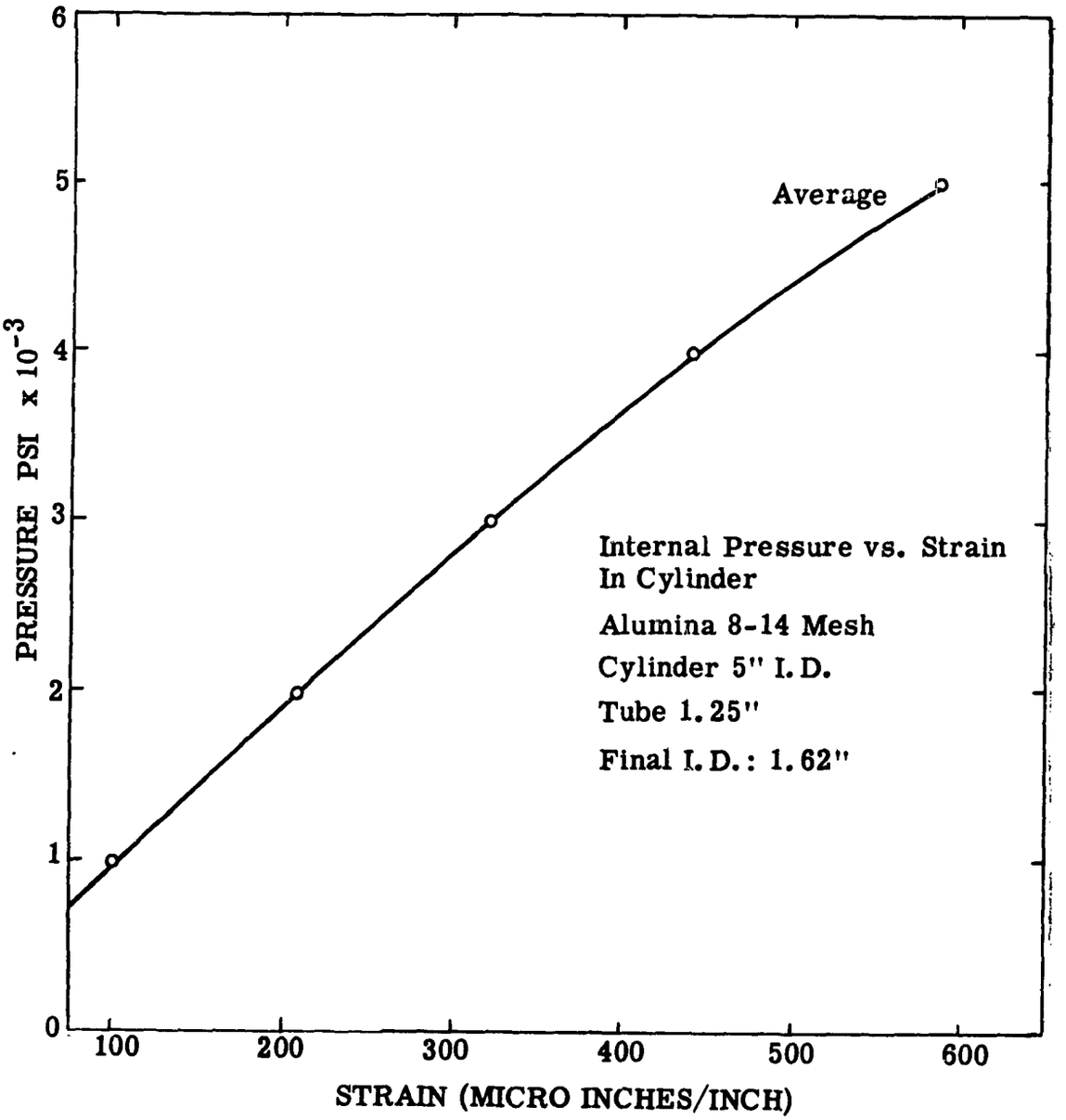
6
5
4
3
2
1
0
PRESSURE PSI x 10^{-3}
100
200
300
400
500
600
STRAIN (MICRO INCHES/INCH)
Average
Internal Pressure vs. Strain
In Cylinder
Alumina 8-14 Mesh
Cylinder 5" I.D.
Tube 1.25"
Final I.D.: 1.62"

FIGURE 13

Further tests on alumina were made using 120 mesh brown alumina abrasive in the 3 inch cylinder. Three consective tests were made with excellent agreement. The results are shown in Figure 14. We do not believe that chemical compositions of the aluminas is responsible for the observed differences. Probably the explanation is due to particle size.

Silicon Carbide. Tests were made with 120 mesh silicon carbide using both the 3 inch and the 5 inch cylinders with various sized rubber tubes. In general the results show that the pressure vs. strain plot is a straight line, and that the results are consistently the same once the material has been packed. In most of the tests the two gauges on opposite sides of the vessel did not give identical results although they each showed straight line relationships. This is likely due to the rubber tube not being exactly concentric with the steel cylinder. The average of the two gauge readings has been used in plotting the curves. Examination with a microscope showed that none of the particles were fractured.

Fig. 15 is a graph of the results of two consecutive runs, with the hysteresis effect clearly shown. It should be noted that once the pressure is attained it must be lowered to less than 100 psi before the hysteresis loop is closed.

Figure 16 shows the average results of a number of tests with the 3 inch and the 5 inch cylinders and with different sized rubber tubes.

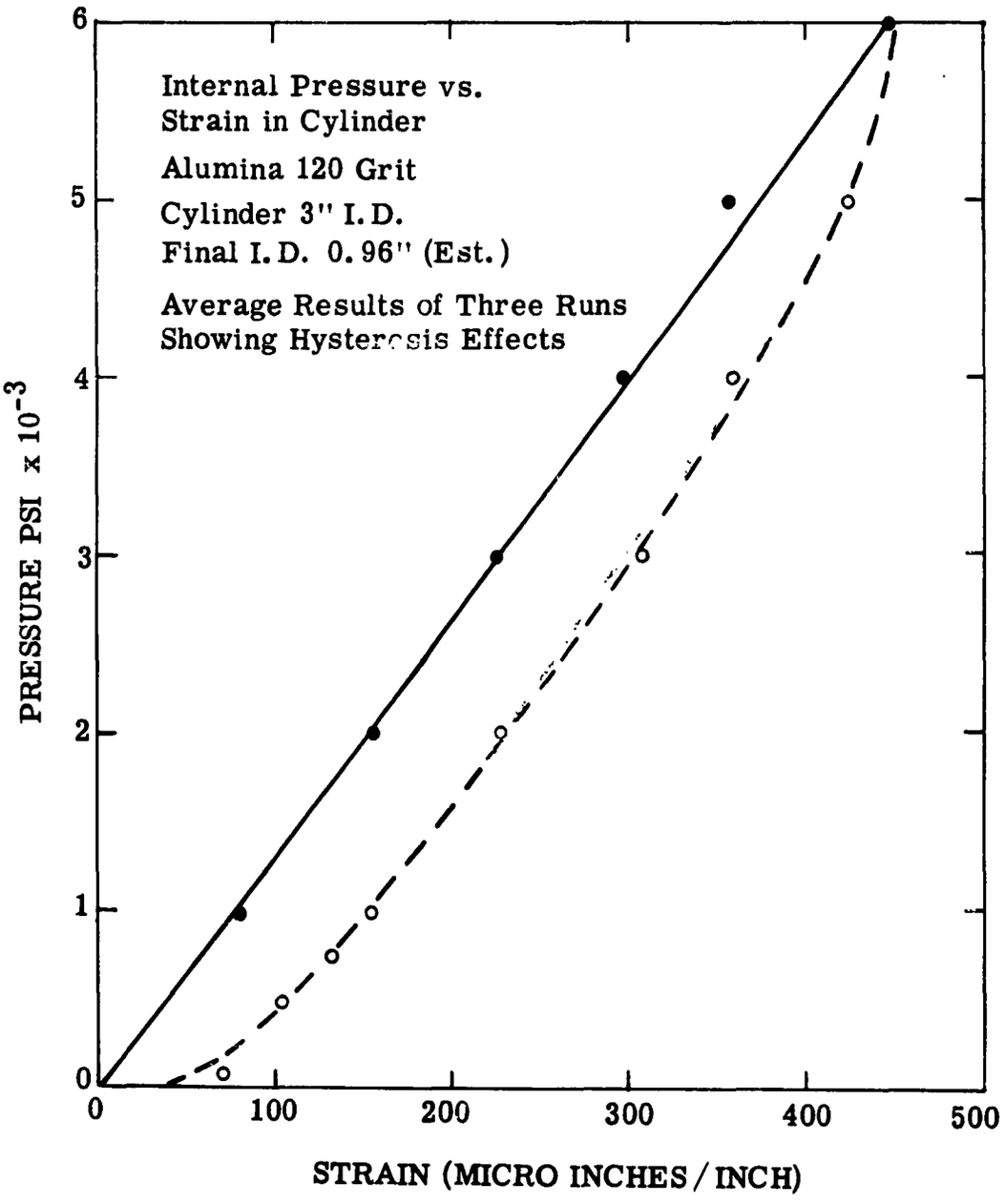
Internal Pressure vs.
Strain in Cylinder
Alumina 120 Grit
Cylinder 3" I.D.
Final I.D. 0.96" (Est.)
Average Results of Three Runs
Showing Hysteresis Effects
PRESSURE PSI x 10^-3
0
1
2
3
4
5
6
0
100
200
300
400
500
STRAIN (MICRO INCHES / INCH)

FIGURE 14

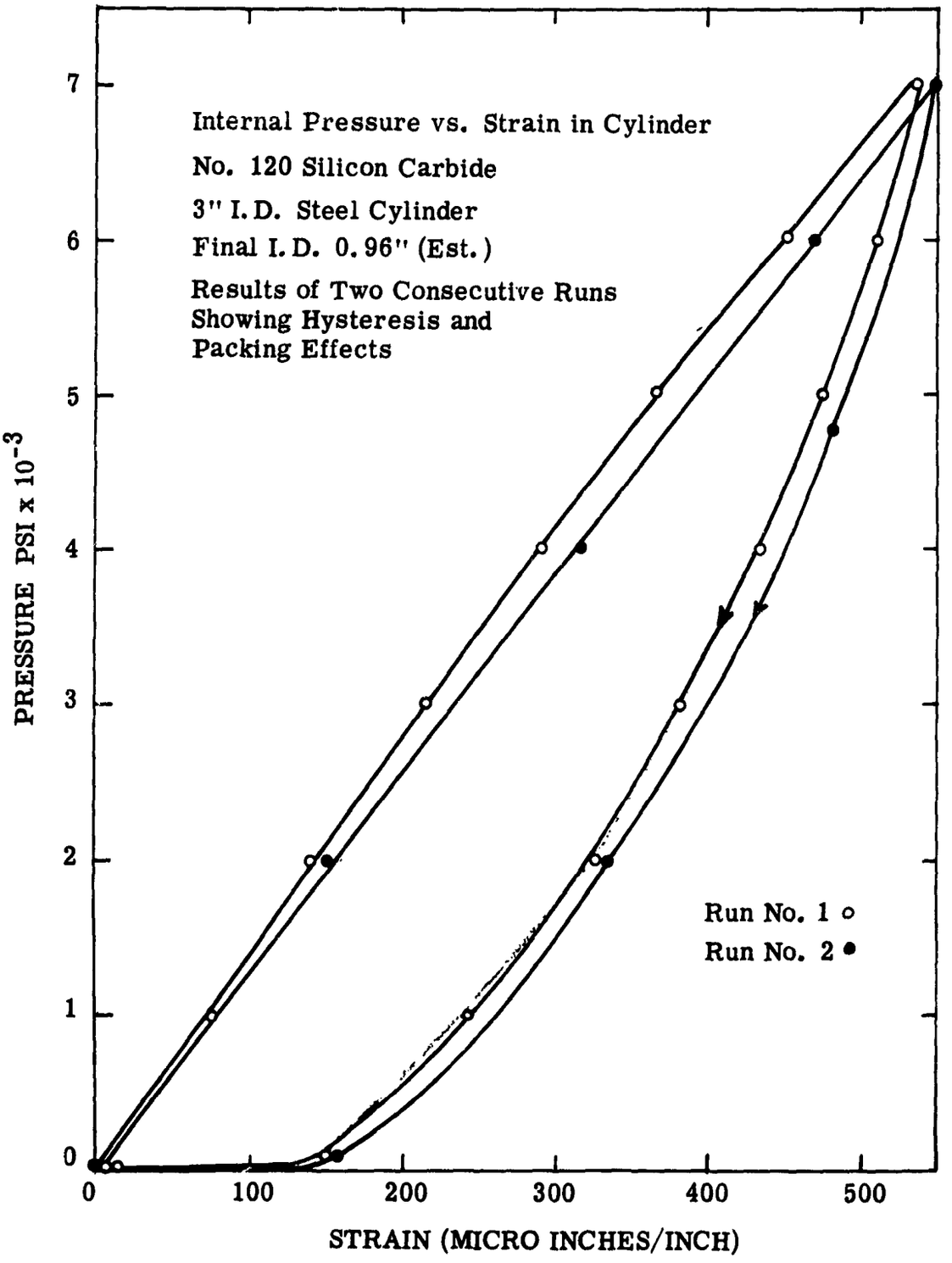
Internal Pressure vs. Strain in Cylinder
No. 120 Silicon Carbide
3" I.D. Steel Cylinder
Final I.D. 0.96" (Est.)
Results of Two Consecutive Runs
Showing Hysteresis and
Packing Effects
Run No. 1 ○
Run No. 2 ●
PRESSURE PSI x 10^{-3}
0
1
2
3
4
5
6
7
0
100
200
300
400
500
STRAIN (MICRO INCHES/INCH)

FIGURE 15

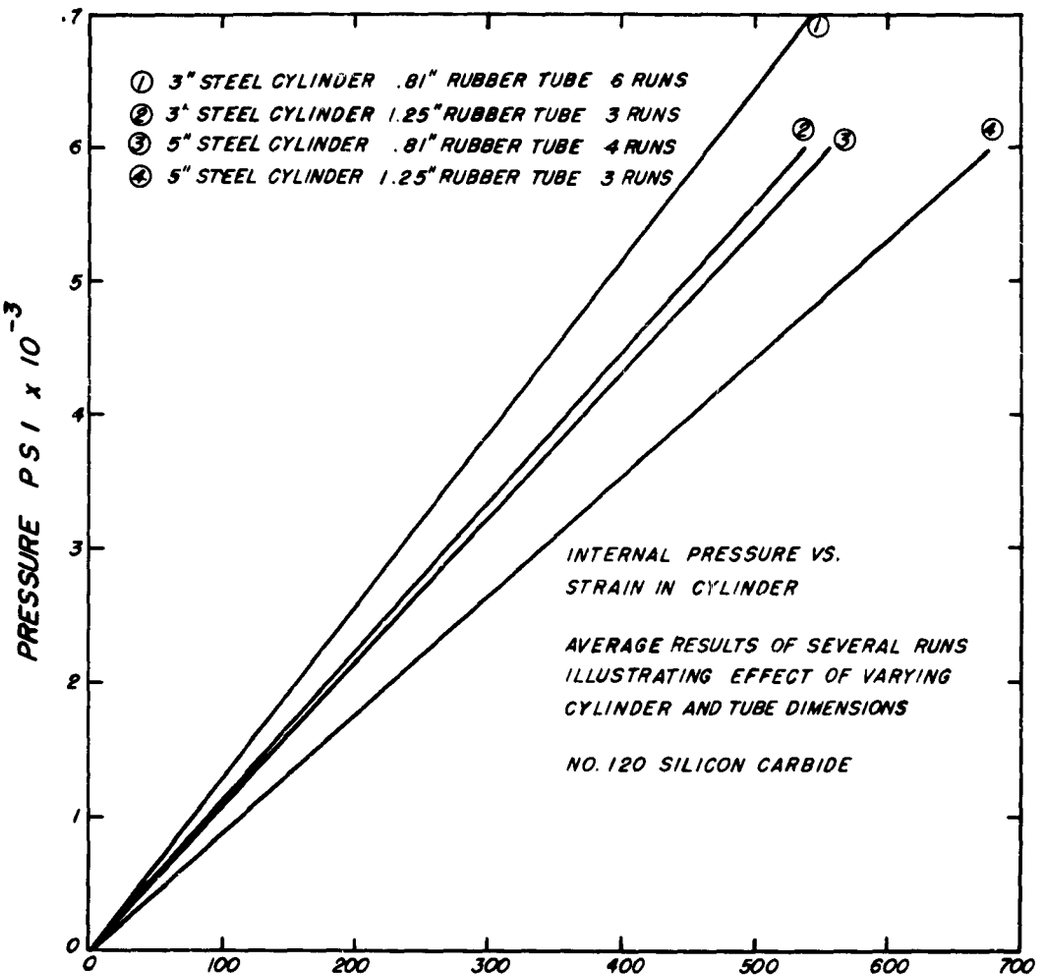
① 3" STEEL CYLINDER .81" RUBBER TUBE 6 RUNS
② 3" STEEL CYLINDER 1.25" RUBBER TUBE 3 RUNS
③ 5" STEEL CYLINDER .81" RUBBER TUBE 4 RUNS
④ 5" STEEL CYLINDER 1.25" RUBBER TUBE 3 RUNS
INTERNAL PRESSURE VS. STRAIN IN CYLINDER
AVERAGE RESULTS OF SEVERAL RUNS ILLUSTRATING EFFECT OF VARYING CYLINDER AND TUBE DIMENSIONS
NO. 120 SILICON CARBIDE
PRESSURE PSI x 10^{-3}
0
1
2
3
4
5
6
.7
0
100
200
300
400
500
600
700
STRAIN (MICRO INCHES/INCHES)

FIGURE 16

Zirconia. The most extensive data obtained in this series of experiments was with 14 F fused zirconia (run of mill with all coarser than 14 mesh screened out). Tests were made with cylinders having inside diameters of 1 1/2 inches, 2 inches, 3 inches, and 5 inches. Rubber tubes 0.85 inches and 1.25 inches OD were used with each steel cylinder. The pressure vs. strain curves are shown in Figures 17 and 18. A hysteresis test was made with one cylinder as follows. The pressure was increased from 0 to 6000 psi obtaining strain readings as the pressure was increased. The pressure was then decreased to 1000 psi and the strain reading showed a higher value than that previously obtained at 1000 psi. The pressure was then increased again and the strain reading did not change until the pressure reached the value which corresponded to this strain in the initial increase in pressure. Further increases in pressure resulted in strain readings duplicating those first obtained. The data obtained from these tests, including the inside diameter as measured by the gamma-graphs, are tabulated in Table 10. The diameters are tabulated at 4000 psi. The pressure was first increased to 6000 psi and then lowered to this value since it was easier to maintain. It is interesting to note that pictures made at 6000 psi and then at 4000 psi showed no detectable change in diameter.

DISCUSSION OF RESULTS

The materials which showed a straight line relationship between pressure and strain were those which showed no fracture when examined

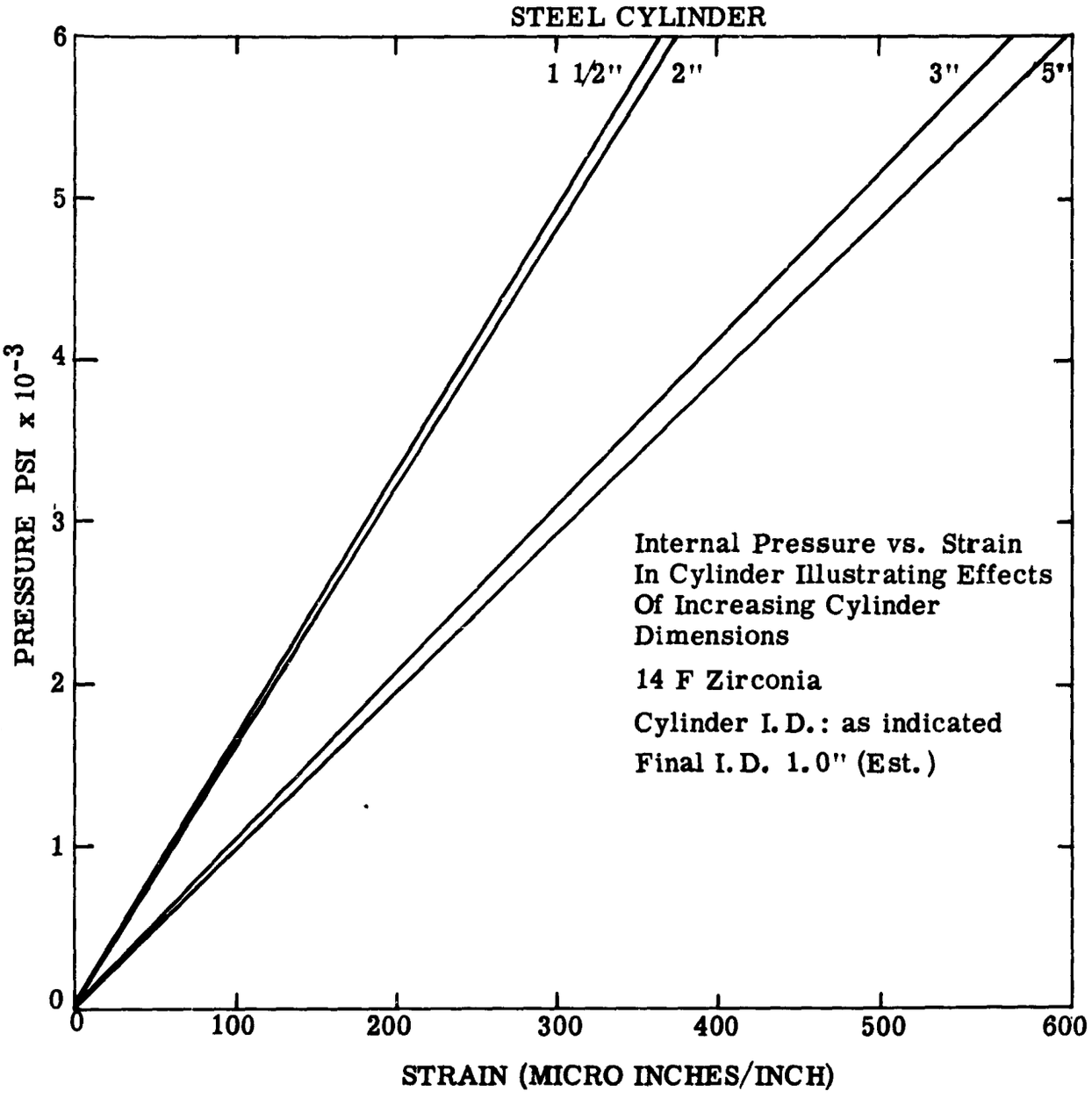
STEEL CYLINDER
1 1/2"
2"
3"
5"
PRESSURE PSI x 10^{-3}
0
1
2
3
4
5
6
0
100
200
300
400
500
600
STRAIN (MICRO INCHES/INCH)
Internal Pressure vs. Strain
In Cylinder Illustrating Effects
Of Increasing Cylinder
Dimensions
14 F Zirconia
Cylinder I.D.: as indicated
Final I.D. 1.0" (Est.)

FIGURE 17

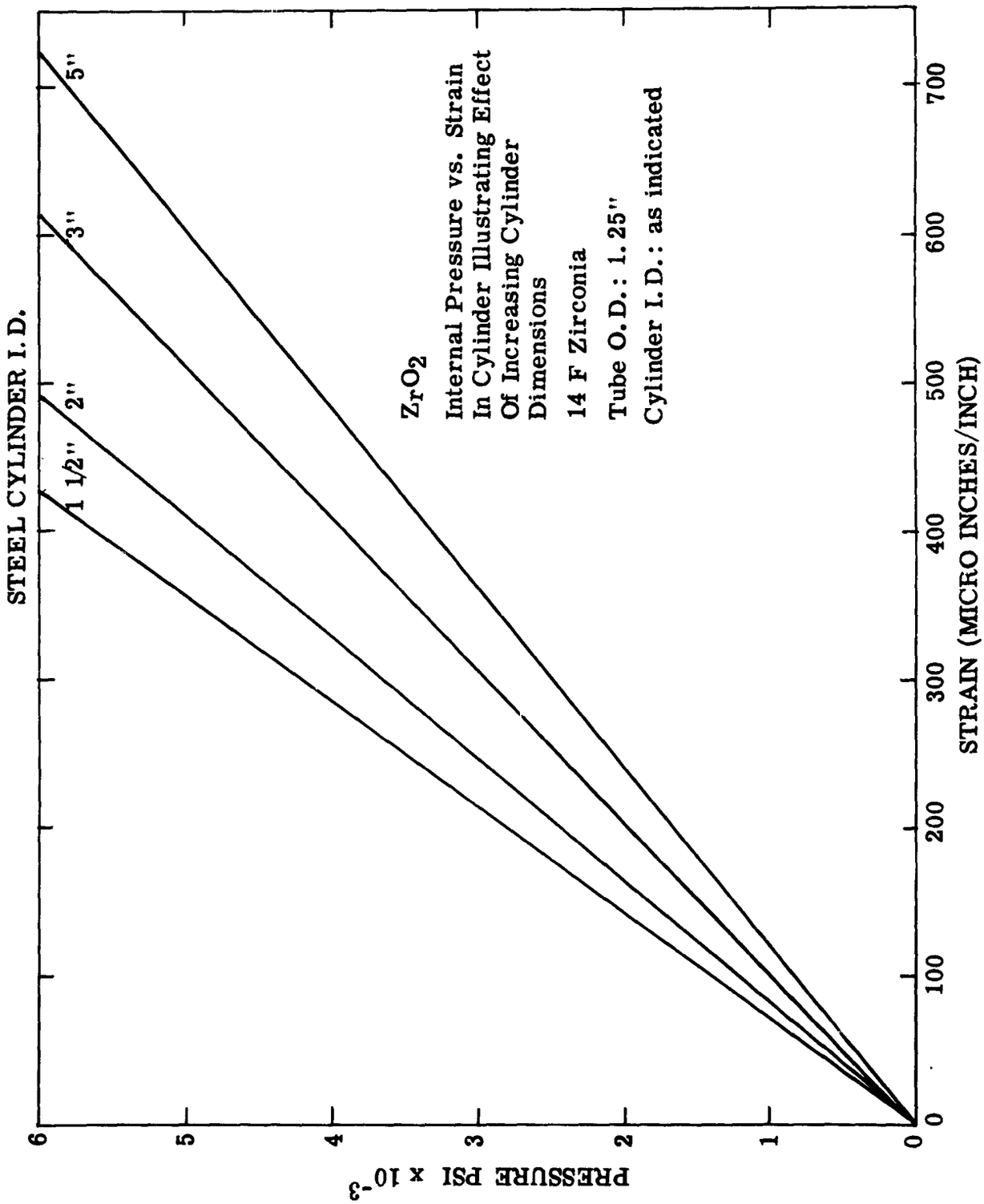
STEEL CYLINDER I.D.
1 1/2"
2"
3"
5"
ZrO_2
Internal Pressure vs. Strain
In Cylinder Illustrating Effect
Of Increasing Cylinder
Dimensions
14 F Zirconia
Tube O.D.: 1.25"
Cylinder I.D.: as indicated
PRESSURE PSI x 10^{-3}
STRAIN (MICRO INCHES/INCH)
0
1
2
3
4
5
6
0
100
200
300
400
500
600
700

FIGURE 18

Table 10

Results of Tests on Zirconia and Silicon Carbide

	1	2	3	4	5	6	7	8	9*
Inside Diameter of Steel Cylinder (inches)	1.500	1.500	1.996	1.996	3.004	3.004	4.995	4.995	3.004
Wall thickness of Steel Cylinder (inches)	.264	.264	.255	.255	.255	.255	.260	.260	.255
O.D. of Rubber Tube (inches)	1.25	.85	1.25	.85	1.25	.85	1.25	.85	.85
I.D. of Z_rO_2 Cylinder from gamma-graphs @ 4000 psi (inches)	1.21?	.925	1.25 ?	.91	1.34	1.14	1.31	1.23	1.02
Strain at 4000 psi micro inches/inches	283	242	332	252	412	390	480	405	357

* #120 Silicon Carbide

with a microscope. This straight line seems to indicate elastic behavior. This elastic behavior would suggest that the conventional Lamé -- Clapeyron equations for the distribution of stress in a thick walled cylinder could be applied to these materials. There is, however, one important detail that must be considered. These equations predict a tensile stress at the inner wall for high internal pressures, which is impossible. Nevertheless, it was thought to be instructive to carry out the computations for stresses in an elastic cylinder with the dimensions, internal and external pressures recorded in Column 5, Table 10, using Equation (2). For this equation, p_i = 4000 psi, a = 0.67" and n = 1.502/0.67 = 2.24. The external pressure, p_0, was calculated by applying the same equation to the steel shell and finding the internal pressure necessary to strain the outside fibers 412 microinches per inch, viz., 2150 psi. Substituting these values into the equation gives $\sigma_t = -1685 + 1035/r^2$, from which the values plotted in Fig. 19 were obtained. It will be seen from this figure that all but a small portion of an elastic body would be under compression. A calculation of total outward thrust from that portion of the curve under the zero stress axis leads to only a small error.

The outward thrust at the center = 1.34 x 4000 = 5360 lbs. while at the steel wall it is 3.004 x 2150 = 6460 lbs., giving a thrust ratio of 1.205. If the granular zirconia were acting as pure columns the ratio would be 1, if it distributed pressure hydrostatically the ratio would be 2.24. It is evident from the data that the zirconia is behaving much more

like columns than like a liquid.

Calculation of the value of Poisson's ratio from a thrust ratio of 1.205 by Equation (8) gives a value of m = 0.57. This seems much too high. Using the more refined Equation (9) leads to an absurd value above 3. Spurious results for a powder using Equation (9) should be expected since the powder can have no tensile stress and, therefore, at any given pressure the granules will so adjust to each other, after the case has expanded, as though the case were perfectly rigid.

Calculation of g in Equation (12) gave 0.22, a not unrealistic value.

The results of experiments on granular materials have, for convenience, been grouped into two parts. In Tables 11 and 12 are found the tests run prior to development of the gamma-graph method of measuring the internal diameters of the powders. Derived quantities from these data will be in doubt because of the uncertainty in the estimation of the ID. Tables 10 and 13 include all data in which ID's were measured by gamma-graphs. The first 8 columns of Tables 10 and 13 report tests on zirconia, the 9th on silicon carbide.

It will be observed that the thrust ratio never sinks below one as it would with an elastic solid. On the other hand, while it increases with n it never approaches that number in magnitude. The ratio of tangential to radial stress, g, averages 0.24 for the data of Table 13. This is what would be expected from a homogeneous solid with a

Table 11

Material	20-30 mesh Ottawa Sand	Sand 3rd Run Fig. 11	Sand Fig. 11 5-6 Run	Coarse Beads 1st Run	8-14 Alumina	120 Alumina
I. D. of Steel Cyl.	3"	3"	3"	3"	5"	3"
I. D. of Powder at 4000 psi, Est.	1.1"	0.96"	0.96"	0.96"	1.62"	0.96"
Strain at 4000 psi micro inches/inch	315	295	370	350	380*	300
n	2.72	2.13	3.13	3.13	3.08	3.13
p_o, psi	1690	1580	1980	1880	1320	1610
T_R	1.15	1.23	1.55	1.47	1.02	1.26
g	0.14	0.18	0.38	0.34	0.02	0.20

* Extrapolated from lower values.

Table 12

Silicon Carbide

Data	Fig. 15 1st Run	Fig. 15 2nd Run	Fig. 16 1st Curve	Fig. 16 2nd Curve	Fig. 16 3rd Curve	Fig. 16 4th Curve
I.D. Steel Cylinder	3"	3"	3"	3"	5"	5"
I.D. Powder at 4000 psi, Est.	.096"	.096"	0.10	1.4"	1.1"	1.4
Strain at 4000 psi micro inches/inch	290	315	310	357	370	450
n	3.13	3.13	3.00	2.14	4.55	3.56
p_0, psi	1550	1690	1660	1920	1280	1560
T_R	1.21	1.32	1.24	1.03	1.45	1.40
g	0.16	0.24	0.20	0.16	0.22	0.26

Table 13

Column	1	2	3	4	5	6	7	8	9
n	1.24	1.62	1.60	2.20	2.24	2.64	3.82	4.06	2.94
p_0 psi	3400	2910	2790	2100	2150	2040	1530	1290	1860
T_R	1.06	1.18	1.12	1.18	1.20	1.35	1.46	1.31	1.37
g	.24	.34	.24	.18	.22	.30	.24	.20	.28

Poisson ratio of 0.2, according to Equation (16), which indicates that granular solids are very good for containing high pressures.

The fact that the thrust ratio, T_R, increases with crushing of the granules can probably be attributed to enlargement of the central hole, though this point will bear further investigation. The data at hand do not make it possible to determine with any certainty the effect of crushed grain vs. well sized or rounded grain. On the other hand, the crushed and unsized zirconia grain shows about the same g as the sized silicon carbide and silica which may indicate that lateral pressure is little influenced by size, shape or packing characteristics. This will be a rather far reaching conclusion if it can be established.

We have no explanation for the wide divergence of the 5th and 6th runs on Ottawa sand from the first four in Fig. 11. From Equation (10) σ_t can be obtained for column 5, of Tables 10 and 13 as $\ln\sigma_t = 0.772 \ln 0.67/r + 2.96$, which is plotted also on Figure 19. We feel that this curve is much more realistic than that calculated from elastic theory.

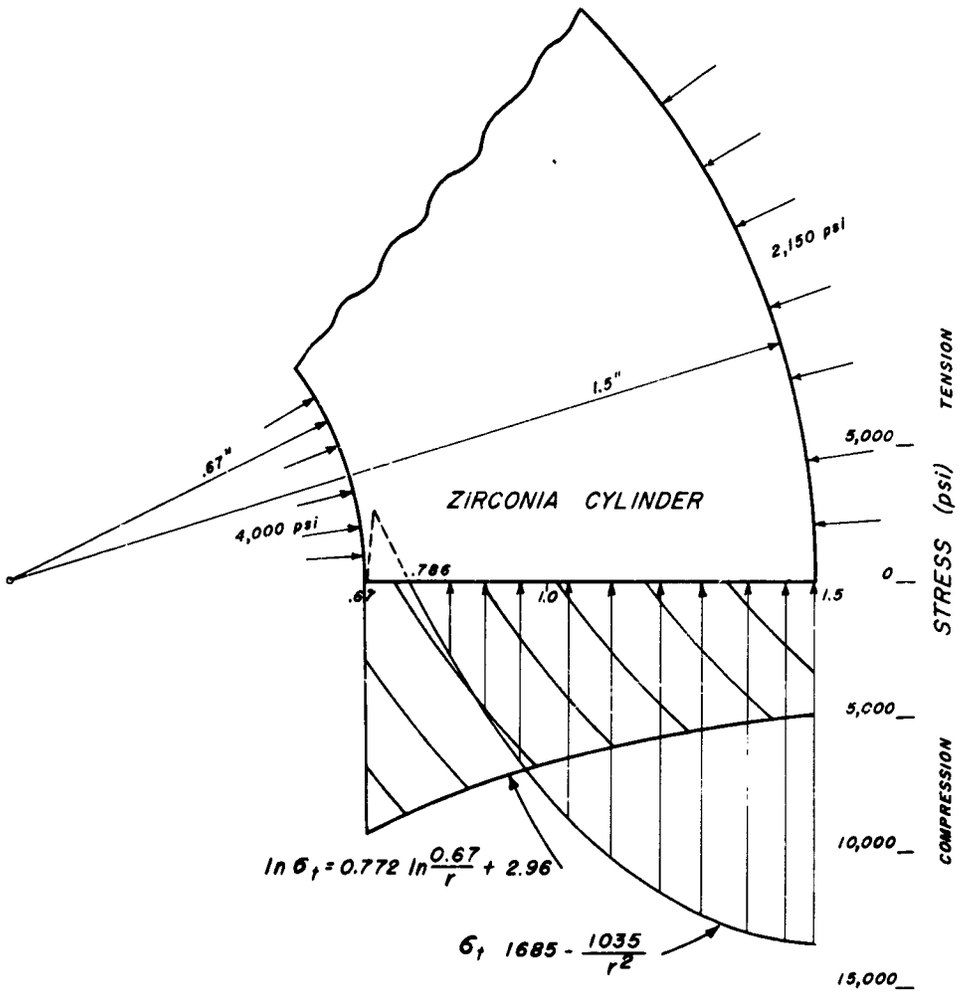

STRESS DISTRIBUTION IN ZIRCONIA CYLINDER

FIGURE 19

The curve for lateral force vs. radius is almost certain to take this form.

CONCLUSIONS

Elastic theory can be very useful in gaining some insight into stresses that may be encountered in vessels designed for extreme pressures. It provides a point of departure for closer approximations that, for the most part, are not subject to exact analysis.

Ultimately high pressures must be retained by tensile members, the design of which can be satisfactorily accomplished for simple cases through elastic theory.

Even weak materials are useful in high pressure design since there is no indication that they will distribute stresses hydrostatically, even when extensively fragmented. Powders support loads much more nearly in a columnar fashion than hydrostatically.

TECHNICAL REPORT DISTRIBUTION LIST
University of Utah
June 15, 1956

Contract Nonr 128802 NR 052-357

No. Copies

Commanding Officer
Office of Naval Research Branch Office
The John Crerar Library Building
86 East Randolph Street
Chicago 1, Illinois (1)

Commanding Officer
Office of Naval Research Branch Office
346 Broadway
New York 13, New York (1)

Commanding Officer
Office of Naval Research Branch Office
1030 E. Green Street
Pasadena 1, California (1)

Commanding Officer
Office of Naval Research Branch Office
Navy #100
Fleet Post Office
New York, New York (2)

Director
Naval Research Laboratory
Washington 25, D.C. (6)
Attn: Technical Information Officer

Chief of Naval Research
Washington 25, D.C.
Attn: Code 425 (2)

Technical Library OASD (R&D)
Pentagon Room 3E1065
Washington 25, D.C. (1)

Technical Director
Research and Development Division
Office of the Quartermaster General
Department of the Army
Washington 25, D.C. (1)

No. Copies

Scientific Director
Quartermaster Research &
Development Command
Natick, Massachusetts (1)

Director
Office of Scientific Research
Air Research & Development
Command
P.O. Box 1395
Baltimore 3, Maryland (1)

Office of the Chief of Ordnance
Department of the Army
Washington 25, D.C.
Attn: ORDTB-PS (1)

Office of Chief of Staff (R&D)
Department of the Army
Pentagon 3B516
Washington 25, D.C.
Attn: Chemical Advisor (1)

Director
Naval Research Laboratory
Washington 25, D.C.
Attn: Chemistry Division (2)

Chief, Bureau of Ships
Department of the Navy
Washington 25, D.C.
Attn: Code 331 (2)

Chief, Bureau of Aeronautics
Department of the Navy
Washington 25, D.C.
Attn: Code TD-4 (2)

TECHNICAL REPORT DISTRIBUTION LIST
(cont.)

Contract Nonr 128802 NR 052-357

	No. Copies
Research Director Chemical & Plastics Division Quartermaster Research & Development Command Natick, Massachusetts	(1)
Director of Research Signal Corps Eng. Laboratories Fort Monmouth, New Jersey	(1)
U. S. Naval Radiological Defense Lab. San Francisco 24, California Attn: Technical Library	(1)
Naval Ordnance Test Station China Lake, California Attn: Head, Chemistry Division	(1)
Office of Ordnance Research 2127 Myrtle Drive Durham, North Carolina	(1)
Technical Command Chemical Corps Chemical Center, Maryland	(1)
Brookhaven National Laboratory Chemistry Division Upton, New York	(1)
Atomic Energy Commission Library Branch Technical Information ORE Post Office Box E Oak Ridge, Tennessee	(1)
Office of Technical Services Department of Commerce Washington 25, D.C.	(1)
Chief, Bureau of Ordnance Department of the Navy Washington 25, D.C. Attn: Code Ad-3	(2)
ASTIA Document Service Center Knott Building Dayton 2, Ohio	(5)
Dr. Francis Birch Department of Geology Harvard University Cambridge, Massachusetts	(1)
Dr. Hatten S. Yoder Geophysical Laboratory 2801 Upton Street, N.W. Washington, D.C.	(1)
Dr. Roland Ward Department of Chemistry University of Connecticut Storrs, Connecticut	(1)
Dr. W. J. Kirkpatrick Mellon Institute Pittsburgh, Pennsylvania	(1)
Institute of Geophysics University of California Los Angeles 24, California Attn: Dr. D.T. Griggs	(1)
College of Mineral Industries Pennsylvania State College State College, Pennsylvania Attn: Dr. O.F. Tuttle	(1)

TECHNICAL REPORT DISTRIBUTION LIST
(cont.)

Contract Nonr 128802

NR 052-357

	No. Copies
Atomic Energy Commission Research Division, Chemistry Branch Washington 25, D.C.	(1)
Commanding Officer Office of Naval Research Branch Office 1000 Geary Street San Francisco 9, California	(2)
Chief of Naval Research Department of the Navy Washington 25, D.C. Attn: Code 423	(1)
Director Naval Research Laboratory Washington 25, D.C. Attn: Dr. Sam Zerfoss	(1)
Dr. Carl J. Christensen University of Utah Salt Lake City 1, Utah	(1)
Dr. S. Young Tyree, Jr. Department of Chemistry University of North Carolina Chapel Hill, North Carolina	(1)